KINALC

A REVIEW OF KINETIC REDUCTION TECHNIQUES AVAILABLE WITH KINALC,

with applications to Methane and Kerosene oxidation

AUTHOR: Anne FELDEN
DATE: September 26, 2013

CERFACS

Tutors: Bénédicte CUENOT

Eléonore RIBER





Abstract

Une présentation des méthodes mathématiques appliquées à la réduction de mécanismes cinétiques chimiques disponibles avec KINALC, et applications aux schémas d'oxydation du Méthane et du Kérosène

Les phénomènes de combustion sont régis par des interactions complexes, faisant intervenir de nombreux processus physiques et chimiques aux temps et longueurs caractéristiques variés. La description fidèle d'un processus chimique nécessite la prise en compte de nombreuses espèces au travers d'un schéma cinétique détaillé. Parfois, comme pour l'oxydation de l'hydrogène, une dizaine d'espèces et une quarantaine de réactions suffisent; mais bien souvent, plus d'une centaine d'espèces en interaction au travers d'un millier de réactions sont nécessaires.

Jusqu'à maintenant, et surtout du fait de la capacité limitée en puissance de calcul, il était d'usage de considérer des schémas dits globaux dans les simulations numériques. Ceux-ci sont constitués d'une ou deux reactions seulement et de moins de cinq espèces. Une telle méthodologie fournit des résultats très satisfaisants pour des quantités générales telles que la température ou la vitesse de flamme; bien que pour un domaine d'applicabilité très limité. Par ailleurs, il faut bien souvent adapter les constantes des réactions impliquées selon les cas considérés. Une alternative existe cependant, qui nécessite de considérer des schémas dits réduits qui fournissent des résultats plus fidèles, grâce à la prise en compte de plus d'espèces et de réactions. De tels schémas se composent d'une dizaine d'espèces et d'une cinquantaine de réactions, et sont aujourd'hui une alternative bien réelle au vu de la capacité toujours grandissante des calculateurs modernes. Ces schémas constituent donc un bon compromis entre une bonne prédictivité et un temps de calcul acceptable.

Une telle réduction de schéma peut être obtenue d'une manière intuitive, a posteriori, en se basant sur l'expérience, ou bien d'une manière plus systématique. Le code open source en FORTRAN 77 KINALC est un outil très utile pour une telle dérivation systématique. KINALC a été développé par des chercheurs de l'Université de Leeds en Angleterre, et de l'Université ETVS à Budapest en Hongrie. Il rend possible l'analyse mathématique et chimique de schémas de réactions au travers, par exemple, de l'analyse des flux atomiques, de l'analyse en composantes principales et de l'analyse des perturbations singulières.

Une description de l'outil KINALC est tout d'abord présentée, illustrée d'un premier exemple de son utilisation sur un schéma d'oxydation du Méthane [21]. Une réduction plus élaborée est ensuite testée sur un schéma d'oxidation du Kérosène [5, 27], complétée par une premire validation du schéma squelette ainsi dérivé.

A review of kinetic reduction techniques available with KINALC, with applications to Methane and Kerosene oxidation

Combustion is a very complex phenomenon, characterized by the interaction and competition of various physical and chemical processes at different time and length scales. Sometimes, the accurate description of chemical reactions can be reached with a detailed kinetic model of 10 species interacting through a 40 reactions scheme (hydrogen oxidation), but often, predictions require hundreds of species interacting through thousands of reactions.

Until recently, and mostly due to computer limited capacity, it was of common practice to use so-called global schemes in numerical simulations, consisting of only one or two reactions and less than five species. Such methodology leads to relatively good prediction of very global features, such as temperature at equilibrium or flame speed, but in a limited application range; and requires the tuning of the reaction constants. An alternative is the so called reduced schemes, which aim at better describing combustion phenomena by retaining more species and reactions in a physically-oriented way. Such schemes, consisting of about 10 species and 50 reactions, are nowadays affordable on the current HP computers, and are a good compromise between CPU time and accuracy.

This reduction can be done in a brute way, using experience and a try-and-error approach, or in a more systematic way. One of the tools that can help to systematic reduction is the open source FORTRAN 77 program KINALC. KINALC was designed by researchers of the University of Leeds in the UK and of the ETVS University (ELTE) in Budapest, Hungary. It can carry out chemical and mathematical analysis of reaction schemes through, for example, Path Flux analysis, Principal Component Analysis, or Computational Singular Perturbation.

A description of KINALC's options is provided, along with a first example of its use on a skeletal Methane / Air combustion mechanism developed by Lu and Law [21]. Next, a more advanced reduction is tested on a Kerosene/ Air combustion mechanism developed by Dagaut [5] and Luche [27], and a first validation of the derived reduced skeletal scheme is performed.

Contents

C	ERF	ACS P	resentation	5				
1	Ger	neral I	ntroduction and State-of-the-Art	6				
2	Obj	Objectives and structure of the present report						
3	Me	Methods of the literature for the reduction of kinetic mechanisms						
	3.1	Introduction						
	3.2	From	detailed schemes to skeletal schemes	10				
		3.2.1	Sensitivity and uncertainty analysis	10				
			Local sensitivities	10				
			Overall sensitivities	11				
			Uncertainty Analysis	12				
		3.2.2	Path Flux analysis (and rate-of-production analysis)	12				
		3.2.3	Lifetime of species	13				
		3.2.4	Principal Component Analysis (PCA)	14				
	3.3 From skeletal schemes to reduced schemes							
		3.3.1	Quasi Steady State Approximation (QSSA)	16				
			QSSA hypothesis and principle	16				
			QSSA error estimation	16				
		3.3.2	$\label{thm:cond} \mbox{Time-scale analysis}: \mbox{Computational Singular Perturbation (CSP)} \ \dots \ \dots \ \dots$	17				
4	Nui	merica	l tools	19				
	4.1	The C	CHEMKIN II package	19				
		4.1.1	General presentation	19				
		4.1.2	Perfectly Stirred Reactor (PSR)	21				
		4.1.3	One dimensional propagating premixed flame (PREMIX)	22				
	4.2	KINA	LC : A program for the kinetic analysis of reaction mechanisms	24				
5	Exa	mple	of reductions with KINALC	2 5				
	5.1		CSP option of KINALC applied to a Methane-Air skeletal scheme to identify QSS s	25				
		5.1.1	Skeletal scheme description and methodology	25				
		5.1.2	Results and conclusion	28				
	5.2		dified KINALC PCAF option applied to a Kerosene-Air skeletal scheme to identify dant reactions	32				
		5.2.1	Skeletal scheme description	32				

		5.2.2	Discussion about the methodology	34
		5.2.3	Semi-Automated PCAF procedure	34
		5.2.4	Modified PCAF option of KINALC, for the detection of $important$ eigenvectors	36
		5.2.5	Results and discussion	37
6	Con	clusio	n	4 1
7	Ann	ıex		42
	7.1	Annex	A: Example of a detailed mechanism, the H2/O2 San Diego mechanism	42
	7.2	Annex	B: A brief KINALC manual	43
	7.3	Annex	C: Automatisation of KINALC post-processing and application to the PCAF option	47
		7.3.1	Summarizing scheme	47
		7.3.2	Modified KINALC driver	48
		7.3.3	Modified PCAF option of KINALC	51
		7.3.4	Link to the python programs (for CERFACS people)	55
	7.4	Annex	D: PSR validation of the skeletal 15/25 PCAF-0.950 mechanism obtained with LC	56
	7.5	Annex	E: PREMIX validation of the skeletal 15/25 PCAF-0.950 mechanism obtained with	65

CERFACS Presentation

CERFACS (Centre Europen de Recherche et de Formation Avance en Calcul Scientifique) is a research organization that aims to develop advanced methods for the numerical simulation and the algorithmic solution of large scientific and technological problems of interest for research as well as industry, and that requires access to the most powerful computers presently available.

CERFACS has seven shareholders:

- CNES, the French Space Agency;
- EADS France, European Aeronautic and Defence Space Company;
- EDF, French Electricity Group;
- Meteo-France, the French meteorological service;
- **ONERA**, the French Aerospace Lab;
- **SAFRAN**, an international high-technology group;
- TOTAL, a multinational energy company.

CERFACS is governed by a *Conseil de Gérance* with representatives from its shareholders, and benefits from the recommendations of its *Scientific Council*.

CERFACS hosts interdisciplinary teams, both for research and advanced training that are comprised of physicists, applied mathematicians, numerical analysts, and software engineers. Approximately 150 people work at **CERFACS**, including more than 130 researchers and engineers, coming from 10 different countries. They work on specific projects in nine main research areas:

- Parallel algorithms,
- Code coupling,
- Aerodynamics,
- Gas turbines,
- Combustion,
- Climate,
- Environmental impact,
- Data assimilation,
- Electromagnetism and Acoustics.

Part of the research activity of **CERFACS** is associated with **CNRS** (Centre National de la Recherche Scientifique), as well as with **INRIA** (Institut National de Recherche en Informatique et Automatique). **CERFACS** participates in **TVE** (Terre Vivante et Espace, pole of laboratories). It is also a member of **RTRA/STAE** (Réseau Thématique de Recherche Avancée "Sciences et Technologies pour l'Aéronautique et l'Espace") and participates in the activities of **AESE** (Pole de Compétitivité "Aéronautique, Espace et Systèmes Embarqués").

1 General Introduction and State-of-the-Art

General Introduction

The emergence of new energy sources in the last 50 years, such as natural gas, nuclear energy and renewable energies, has significantly decreased the need for fossil fuels in the industrial sector as well as in the tertiary sector. Nonetheless, its need in the transport sector continues to increase, due to both a lack of substitute source and increasing population. In 2011, this sector alone accounted for 70% of the final global petroleum consumption.

Unfortunately, combustion of such fuels releases pollutant species such as oxides of carbon (CO, CO_2) , oxides of nitrogen (NO_x) , oxides of sulfur and soot, which are a major worldwide concern. The priority has been leaning towards a reduction of this negative impact, by keeping in mind that a substitute energy source for transport is not an option in the foreseable future. In this context, there is considerable demand to improve efficiency while reducing consumption and emissions for the next generation of combustion technology. Additionally, a drastic reduction of both development and experimental costs of new technologies is today required.

Mostly due to this latter consideration, numerical simulation drives the design in the transport industry. Recent advances in reacting Reynolds-Averaged Navier Stokes (RANS) and Large Eddy Simulation (LES) [52, 36], coupled to the increasing available computational power, now allow realistic simulation of rather complex devices. Furthermore, turbulence phenomena as well as its interaction with combustion are nowadays better understood and very accurately predicted. Comprehensive flame chemistry, on the other hand, is a rather new field of research. Traditionally, the inclusion of chemical kinetics in practical combustion simulations used one or multi-step semi-global reactions, to decrease both the required computational time and the mechanism's stiffness that the use of a detailed scheme of sometimes over a thousand reactions would induce. As such, reaction schemes are completely devoid of chemistry and only reproduce global quantities such as flame speed and burnt gas state.

In recent years, efforts have been made towards a more accurate inclusion of chemistry in most reduced schemes, mostly through the use of the In Situ Adaptive Tabulation method [9], which acts as a chemical "library" throughout the combustion simulation. Such a method has obvious drawbacks, the most important ones being the increasing computational weight of the libraries with the complexity of the configurations, along with the library determination in certain delicate cases. The latest approach considered in the community makes use of analytically derived reduced schemes, which are self sufficient in that they do not require adaptation to particular cases inside their respective parameter range. Such schemes are typically composed of under 50 global reactions, and cleared off of any stiffness source.

In view of the previous discussion, and in order to make the numerical simulation of reactive flow computationally affordable and comprehensively accurate, the development of computational approaches for rigorous reduction of detailed mechanisms is today essential.

State-of-the-Art in the derivation of detailed kinetic schemes

Two different types of reduction can be performed on a detailed scheme, depending on its initial size as well as on the phenomena to reproduce.

- A *skeletal reduction* will produce a skeletal scheme from a detailed one, by simply discarding a set of "unnecessary" species and reactions.
- An analytical reduction will produce a reduced scheme either from a skeletal scheme, or sometimes directly from the original detailed one, by combining the remaining reactions and associated reaction rates.

Both reductions have their respective tools and techniques, an overview of which is provided hereafter in table 1. The most common procedure for the skeletal reduction, is to begin by the identification and elimination of *redundant* species (and associated reactions) followed by the identification and elimination

Skeletal reduction	Analytical reduction
Identification of the redundant species	Fast species identification
Sensitivity and Uncertainty Analysis [42]	Computational Singular Perturbation Analysis (CSP)
Path Flux Analysis	Lifetime analysis
Directed Relation Graph Analysis (DRG)	Reaction rate criteria [2]
Jacobian investigation [43]	
Identification of the redundant reactions	Differential equations simplification techniques
Sensitivity and Uncertainty Analysis	Truncation [35]
Principal Component Analysis (PCA) [42]	Partial Equilibrium (PE) [38, 39]
Frenklach Method	Intrinsic Low-Dimensional Manifolds (ILDM) [9, 29, 30]
	Inner iteration (chapter 6 in [35])

Table 1: Common kinetic scheme reduction techniques. Further references can be found in section 3.

of redundant reactions (terminology from [43]). The analytical reduction then deals with the eradication of the stiffness from the mechanism, mostly through equilibrium approximations and truncation of the reaction rate of so-called fast species, followed by equations recombination, and sometimes simplifications.

Typically, the size of a detailed mechanism increases with the carbon atoms number and, usually, the heaviest hydrocarbon mechanisms rest strongly on lighter hydrocarbon mechanisms [4, 18], from which they derive their main features. It explains, in part, why focus of the last century has mainly leaned towards the derivation of reduced schemes for lighter hydrocarbon oxidation, such as hydrogen (e.g., in [1, 35] or [33, 37] revised in [4, 19]) or methane oxidation [7, 21]. Since these are of reasonable size to begin with, a number of reduction techniques rely strongly on "chemical intuition" and experience [10] -as it is often the case for the sensitivity and uncertainty analysis. However, such techniques are not well suited to the study of heavier hydrocarbon oxidation mechanisms; and this fact, coupled with the growing need for comprehensive chemical schemes outside of the "pure chemistry" community, has contributed to the emergence of purely mathematical reduction tools, such as CSP, ILDM or PCA (see table 1). Such tools are furthermore naturally well designed for numerical implementation in preexisting chemistry or combustion simulation codes, usually as post processors, e.g. in CARM [3], the S-STEP [31], or more recently, the G-scheme [51]. Such codes are able to both carry the model reduction and perform the subsequent numerical integration of the derived set of differential equations, thus simplifying the crucial validation step.

The trend today is towards a systematical reduction of any detailed chemical scheme, without any prior chemistry knowledge.

2 Objectives and structure of the present report

In the six months that I have spent at CERFACS, I have performed several tasks allowing me to work and develop competencies in various fields. I were given the opportunity to work in a research environment, and that meant that I could be autonomous in my work and beneficiate from senior researchers' and PhD students' experience.

The first two months were dedicated to getting started with the open source FORTRAN 77 code KINALC, and the exploration of its several options. KINALC had never been used by the people of CERFACS previously, therefore I had to find all information and documentation available in the literature. In parallel, I had to learn how to use the CHEMKIN-II package (see section 4.1), an old version of the chemistry simulation tool CHEMKIN, written in FORTRAN 77 and used by KINALC. Indeed, the different options available had not been used by CERFACS members for a long time, as new chemical codes are now available in the community, and "I" (with the precious help of Carmen JIMENEZ!) had to perform some minor alterations on the code while launching a series of elementary tests to validate it. Sections 3 and 4 of the present report summarize the gathered information on KINALC and CHEMKIN-II, as well as on the theory behind those numerical tools, and a brief KINALC list of keywords and options is given in Annex B.

The third month was dedicated to further testing KINALC options, which were mainly performed on methane-air combustion already used as a reference at CERFACS. Ultimately, KINALC was used to reduce the detailed GRIMECH 3.0 mechanism to a skeletal mechanism close to the existing Lu and Law [24] scheme. The results are presented in section 5.1.

During the last months, I first developed competencies in shell script and python programming, in order to efficiently post-process the results from KINALC. Indeed, in order to reduce any mechanism, a series of academic calculations is launched on a broad range of configurations, and it takes a rather long time to process an post-process the results of each calculation. Second, a more efficient methodology was adapted for one of the most useful option of KINALC, and tested on a Kerosene-Air skeletal mechanism [27] - derived from a detailed one [5], in order to rapidly obtain a smaller skeletal scheme. The proposed way of proceeding follows closely the idea and methodology of [18] and [27], and is further described in section 5.2.2.

Finally, the KINALC derived Kerosene-Air skeletal scheme was compared to skeletal schemes presented in [27], and tested on various configurations, as an attempt to validate it. A discussion on the results is presented in section 5.2.5, and details regarding the coding and the technical aspects of the methodology can be found in Annex C.

3 Methods of the literature for the reduction of kinetic mechanisms

3.1 Introduction

The numerical simulation of combustion system relies on the accurate description of n chemical species interacting through a series of m elementary reactions ([36, 54]):

$$\sum_{1 \le i \le n} \nu'_{ij}[X_i] \rightleftharpoons \sum_{1 \le i \le n} \nu''_{ij}[X_i], \quad for \quad j \in [1, m]$$

$$\tag{1}$$

where $[X_i]$ stands for species i molar concentration and ν'_{ij} and ν''_{ij} are the molar stoichiometric coefficients of species i in each side of reaction j. In homogeneous mixtures, combustion relies on the evaluation of the following initial value problem (for example, in [50]):

$$\frac{d\mathbf{c}(\mathbf{c}, \mathbf{k})}{dt} = \mathbf{f}(\mathbf{c}, \mathbf{k}), \quad \mathbf{c}(t_0) = \mathbf{c_0}$$
 (2)

where \mathbf{c} is the molar concentration vector of dimension n, \mathbf{k} is the vector of reaction rate coefficients of dimension m and $\mathbf{c_0}$ are the initial molar concentrations. Only the concentration vector has time dependence.

The right hand side of Eq. (2) can also be calculated from the rates of each forward and backward j reaction $R_j(\mathbf{c}, k_j) = k_{fj} \prod [X_k]^{\nu'_{kj}} - k_{rj} \prod [X_k]^{\nu''_{kj}}$ as well as from the global molar stoichiometric coefficients of species i in the j-th reaction $\nu_{ij} = \nu''_{ij} - \nu'_{ij}$, as follows ([36, 54]):

$$f_i(\mathbf{c}, \mathbf{k}) = \sum_{0 < j < m} \nu_{ij} R_j \tag{3}$$

The forward j-th reaction rate is expressed in the general Arrhenius form:

$$k_{fj} = A_{fj} T^{n_j} exp\left(\frac{-Ea_j}{RT}\right) \tag{4}$$

where T is the temperature, A_{fj} is the pre-exponential factor, n_j is the temperature exponent and Ea_j is the activation energy. R is the universal gas constant.

The backward j-th reaction rate k_{rj} is computed from the forward reaction rate, and the pressure equilibrium K_{pj} constant according to :

$$k_{rj} = \frac{k_{fj}}{\left(\frac{p_0}{RT}\right)^{\sum_{1 < k < n} \nu_{kj}} exp\left(\frac{\triangle_r S_j^0}{R} - \frac{\triangle_r H_j^0}{RT}\right)}$$
(5)

where \triangle_r stands for an enthaply (H) or entropy (S) variation between the products and the reactants of the j-th reaction, and p_0 is the standard atmospheric pressure (1 bar).

The mathematical analysis of the terms composing the ODE system of Eq. (2) gives detailed information on the chemical kinetics, and leads to a better understanding of reaction phenomena. Most used techniques are presented in this section. A difference is made between techniques that allow to obtain a skeletal scheme from a detailed one, and those that allow to obtain a reduced scheme from a skeletal one.

3.2 From detailed schemes to skeletal schemes

3.2.1 Sensitivity and uncertainty analysis

Sensitivity analysis allows to determine which parameters contribute most to the solution variability and thus have to be known with the best possible accuracy to reproduce the correct system behavior. Both local and global sensitivities are defined subsequently.

Local sensitivities

Concentration sensitivities The sensitivity analysis method investigates the output of a system at time t_2 , responding to a modification of the input occurring at time t_1 (either controlled or not), with $t_1 < t_2$. Usually, input modifications are rather small, so as to have an idea of the variability of the system. Local sensitivity is defined as the partial derivative of the output quantity of interest with respect to the modified input ([11, 46]).

In chemical kinetics, the objective is to evaluate the effect of modifying the reaction rates on the species concentration. The following matrix, called the *concentration sensitivity matrix*, is then built as:

$$\mathbf{S} = \frac{\delta \mathbf{c}(t_2)}{\delta \mathbf{k}(t_1)} = \left(\frac{\partial c_i}{\partial k_j}\right)_{ij} \tag{6}$$

Using a Taylor development and neglecting high order terms, the following formula is obtained for each species i, estimating the variation $\triangle c_i$ induced by a variation of $\triangle k$ around the initial input value:

$$\triangle c_i(t_2) \approx \sum_j \frac{\partial c_i}{\partial k_j} \triangle k_j(t_1)$$
 (7)

Or in a matrix form:

$$\triangle \mathbf{c}(t_2) \approx \mathbf{S} \bullet \triangle \mathbf{k}(t_1) \tag{8}$$

The first order partial derivatives are referred to as first-order local concentration sensitivity coefficients [44]. They can be estimated by CHEMKIN-II and post-processed with KINALC.

Often, as it is more convenient to deal with dimensionless quantities, the sensitivity matrix is normalized, by the factor k_j/c_i . The resulting **S** matrix is then defined as:

$$\mathbf{S} = \frac{\partial \ln(\mathbf{c})}{\partial \ln(\mathbf{k})} \tag{9}$$

Eq. (9) represents the relative concentration change of species i at time t_2 caused by an input variation at time t_1 .

Rate-of-production sensitivities Sensitivities of the (net) rate-of-production of species i to a perturbation in the input rate of production j is similarly defined as a rate-of-production sensitivity matrix \mathbf{F} :

$$\mathbf{F} = \left(\frac{\partial f_l}{\partial k_j}\right)_{lj} \tag{10}$$

or equivalently, in a normalized way:

$$\mathbf{F} = \frac{\partial ln(\mathbf{f})}{\partial ln(\mathbf{k})} \tag{11}$$

Here also, small perturbations around an initial input value are considered.

Differentiating Eq. (2) with respect to the j-th reaction rate and inverting differentiating order gives:

$$\frac{\partial f_l(\mathbf{c}, \mathbf{k})}{\partial k_j} = \frac{\partial}{\partial k_j} \left(\frac{dc_l(\mathbf{c}, \mathbf{k})}{dt} \right) = \frac{d}{dt} \frac{\partial c_l(\mathbf{c}, \mathbf{k})}{\partial k_j} = \sum_{0 < i < n} \frac{\partial f_l(\mathbf{c}, \mathbf{k})}{\partial c_i} \right) c_{f \neq c_i \, cst;} \frac{\partial c_i}{\partial k_j} + \frac{\partial f_l(\mathbf{c}, \mathbf{k})}{\partial k_j} c_{f \neq k_j \, cst} (12)$$

An finally, introducing the Jacobian $\mathbf{J} = \mathbf{J}_{lj} = \left(\frac{\partial f_l}{\partial c_j}\right)_{lj}$ gives the following decomposition:

$$\frac{d\mathbf{S}}{dt} = \mathbf{J} \bullet \mathbf{S} + \mathbf{F} \tag{13}$$

It is worth mentioning that when considering an irreversible mechanism, the normalized rate-of-production sensitivity matrix (normalized by the factor k_i/f_l) reads:

$$F_{lj} = \frac{\nu_{lj} R_j}{\sum_{0 < j < m} \nu_{lj} R_j} \tag{14}$$

Overall sensitivities

Overall concentration sensitivities When performing an overall sensitivity analysis, the effect of an input variation at time t_1 is evaluated at a later time t_2 on a subset of output quantities simultaneously. In chemical kinetics typically, it is interesting to assess the effect of a variation of the j-th reaction coefficient on the concentration / production rate of several species. Indeed, changing the value of one input will affect the entire system, and it is important to look at its global response.

This effect can be interpreted through an objective function, defined as the sum of the squares of normalized S (or F) column elements:

$$B_j = \sum_{1 \le i \le n_i} \left(\frac{\partial \ln c_i}{\partial \ln k_j} \right)^2 \tag{15}$$

The summation runs over the indices of the n_i species of interest.

Now, this summation only accounts for the response of the system to a localized perturbation. To account for the time evolution of the system, however, the matrix S (or F) may be evaluated at various time points t_s , $s \in [1, q]$, leading to a "time-averaged" objective function (for n_I species of interest):

$$B_j = \sum_{0 < t_s < q} \sum_{0 < i < n_I} \left(\frac{\partial \ln c_{i,t_s}}{\partial \ln k_j} \right)^2 \tag{16}$$

Overall Jacobian sensitivities Similarly, it is possible to perform an overall sensitivity analysis on the Jacobian:

$$\mathbf{BJ}_{i} = \sum_{0 < l < n} \left(\frac{\partial \ln f_{l}}{\partial \ln c_{i}} \right)^{2} \tag{17}$$

This type of analysis provides an estimate of the effect of the concentration of a species i on the production rate of several species. Evaluating \mathbf{BJ}_i coefficients for different species i, it is possible to rank them, so as to have an idea of the *most important* species (the ones with the highest coefficient value).

However, these coefficients only reflect the *direct* effect of species i on the set of necessary species, and do not provide any information about *indirect* links between species. Indeed some species may affect the necessary species because they affect the species directly linked to them. For that reason, it is recommended to iterate on the evaluation of $(\mathbf{BJ}_i)_i$, in a process described in [43] and in [18]. It is also more efficient to couple the evaluation of \mathbf{BJ} with a method such as the Directed Relation Graph method [26, 34] or the multi-generation Path Flux Analysis method [40] (see section 3.2.2).

Uncertainty Analysis

Uncertainty analysis constitutes a field of research on its own, and it is not the objective of this review to be particularly thorough, as it will be of little interest in what follows. For a detailed review of available techniques and applications, see ([11, 44, 45, 55]).

A system can be sensitive to an input parameter in two different ways. First, the variability or uncertainty associated with a sensitive input parameter can propagate through the model to ultimately have a large contribution to the overall output variability. Second, the output of a system can be highly correlated with an input parameter, so that a small variation of its value results in a large output change. This latter phenomenon is the one investigated by the sensitivity analysis presented before, but such analysis does not tell anything about the parameter importance, or role in the output variability. Indeed, a sensitive input parameter can be controlled accurately, so that its contribution to the output variability will ultimately be insignificant. Parameters that have key roles on output variability are referred to as important parameters.

Numerous different mathematical theories exist, which aim at quantifying the output variability in terms of important input parameters ([11, 45]). They all require that the modeler has an idea *a priori* of the input parameter variability, and all methods of analysis finally identify the same "most sensible" input parameters [11].

One of the frequently used method in the literature is the *direct method*, which uses the *semi-normalized* sensitivity concentration matrix \mathbf{S}^* (the original \mathbf{S} matrix is only normalized by k_j) to calculate the error propagation (for example, in [11, 55]):

$$V(c_i) = \sum_{0 < j < m} \left(\frac{\partial c_i}{\partial \ln k_j}\right)^2 V(\ln k_j)$$
(18)

where V stands for the concentration variance of species i, which can be seen as a local evaluation of uncertainties in model predictions. The method is only valid for small uncertainties.

Using this approach we can consider the terms in the sum, $V_j(c_i)_j$, to be individual contributions from each reaction to the total uncertainty of the concentration of species i. They are also often presented as percentages, following:

$$V_j(c_i)\% = \frac{V_j(c_i)}{V(c_i)} \times 100$$
 (19)

3.2.2 Path Flux analysis (and rate-of-production analysis)

To reduce a kinetic scheme, the knowledge of the chemical path followed by the elements through species during reactions is essential. A simple way of gathering information is done by investigating the way species are connected through the reaction network, by ranking the contribution of each reaction steps to the rate of production of the *necessary* species ¹. This method is referred to in the literature as rate-of-production analysis, and is commonly used to identify *necessary* reactions.

Prior to this is the identification of necessary species steps. A common method deals directly with elements pathways, since if species concentrations evolve in the system during the reaction, the elements concentrations remain constant. Then, elements can be viewed as unbiased markers and provide valuable information on how the species are connected. Moreover, they can help to quantify those connections so as to identify unimportant species, isolated groups of species, or Quasi Steady State (QSS) candidates.

The atomic flux of an element A from species i to species i' through reaction j is expressed as in [8]:

$$\phi(A,j)_{i->i'} = \frac{R_j n_{A,i} n_{A,i'}}{N_{A,j}}$$
 (20)

¹The necessary species are those species without which an accurate description of the considered reaction phenomena (to be defined) cannot be reached

where R_j is the (net) j-th reaction rate, $N_{A,j}$ is the total number of atoms A in the right hand side of reaction j and $n_{A,i}$ (resp. $n_{A,i'}$) stands for the number of atoms A in the species i (resp. i'). The flux of an element A from species i to species i' is usually corrected by the flux from species i' to species i, leading to the net atomic flux:

$$\phi(A,j)_{i->i'}^{net} = \phi(A,j)_{i->i'} - \phi(A,j)_{i'->i}$$
(21)

By taking into account all the reactions j in the mechanism, it is possible to know, at a specified time t, the fluxes of every elements in the system exchanged by two species i and i' in the system. From there, two other broadly used quantities are the sum of the net (positive) fluxes from every species i in the system to a species i', and the sum of the net (positive) fluxes from a species i' to every other species i in the system:

$$\phi(A)_{i'}^{+} = \sum_{0 \le i \le n} Max(\phi(A)_{i->i'}^{net}, 0)$$
(22)

$$\phi(A)_{i'}^{-} = \sum_{0 \le i \le n} Max(\phi(A)_{i'->i}^{net}, 0)$$
(23)

They are referred to, respectively, as the *incoming* and *outgoing* fluxes of element A from species i'. An accurate estimation of species interaction throughout the reaction process is given by integrating the incoming and outgoing atomic fluxes over the whole time interval [18] (see fig. 1 for example):

$$\Phi(A)_{i'}^{\ +} = \int \phi(A)_{i'}^{+} \cdot dt \tag{24}$$

$$\Phi(A)_{i'}^{-} = \int \phi(A)_{i'}^{-} \cdot dt \tag{25}$$

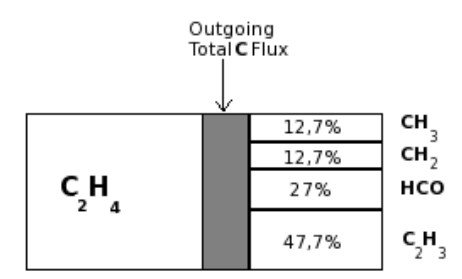


Figure 1: Example of a schematic diagram of an integrated outgoing Carbon flux from species C_2H_4 , to species CH_3 , CH_2 , HCO and C_2H_3 [18].

For each element, those total fluxes are normalized by the total outgoing fluxes of the provider species, so that the most significant fluxes are easily identified, while those lower than a specified threshold can be used to discard associated species and reactions to simplify the scheme [18].

It is also possible, in a latter reducing step, to substract the total outgoing fluxes from the incoming one $\Phi(A)_{i'}^{\ +} - \Phi(A)_{i'}^{\ -}$ for one particular species i' with small total fluxes, and if it is close to zero, to assume it as a QSS species.

3.2.3 Lifetime of species

The species involved in the chemical mechanism each have a specific chemical lifetime, defined, for a molecule of species i, as the time elapsed from its creation to its consumption. It is usually dependent upon other species concentration and temperature, and can differ from several orders of magnitude between species. Those with the shortest overall lifetimes are usually highly reactive chemicals, and could

be potentially QSS species.

A generalized interpretation of the lifetime can be based on the diagonal elements of the Jacobian:

$$\tau_i = -\mathbf{J}_{ii}^{-1} \tag{26}$$

Eg. (26) will be used in further discussion, as it is the definition of species lifetime used by KINALC.

3.2.4 Principal Component Analysis (PCA)

The Principal Component Analysis method is a pure mathematical tool, aiming at reducing the dimensionality of a system by finding a reduced set of variables that will retain most of the original information. In chemical kinetics, such analysis allows to draw conclusions from sensitivity matrices, even with limited knowledge of chemical phenomena. Ultimately, it gives a way to select a minimum set of *important elementary reactions*, as well as a set of potential QSS species, by investigating the effect of reaction parameter change on all species simultaneously. In that sense, it is useful for both skeletal and reduced scheme construction.

The basic concept in PCA lies behind the definition of an objective response function Q, whose formulation depends on the quantity monitored. To estimate, for instance, the response of the concentration of a subset of n_I species i to a perturbation of the vector \mathbf{k} , the following expression -evaluated at different time points $t_s, s \in [0, q]$, is used:

$$Q(\mathbf{k}) = \sum_{0 < t_s < q} \sum_{0 < i < n_I} \left(\frac{c_{i,t_s}(\mathbf{k}) - c_{i,t_s}(\mathbf{k_0})}{c_{i,t_s}(\mathbf{k_0})} \right)^2$$

$$(27)$$

where $\mathbf{k_0}$ is the initial value of \mathbf{k} .

Using a Taylor expansion around $\mathbf{k_0}$ and neglecting the higher-order terms leads to an approximate response function [50]:

$$Q(\mathbf{k}) = (\triangle \mathbf{k})^T \tilde{S}^T \tilde{S}(\triangle \mathbf{k})$$
(28)

where \tilde{S} stands for the q (q different time points) stacked S concentration sensitivity matrices.

The PCA method consists in diagonalizing the $\tilde{S}^T\tilde{S}$ $(m \times m)$ matrix, in order to express it in a $P\Lambda P^T$ form, where the columns of P are normed eigenvectors associated with the eigenvalues of the diagonal matrix Λ . This introduces a new set of variables, or *principal components* (by a change in coordinates):

$$\mathbf{\Psi} = P^T \mathbf{k} \tag{29}$$

Eq. (28) then writes:

$$Q(\mathbf{k}) = (\Delta \mathbf{k})^T P \Lambda P^T (\Delta \mathbf{k}) = (P^T \Delta \mathbf{k})^T \Lambda (P^T \Delta \mathbf{k}) = (\mathbf{\Psi})^T \Lambda \mathbf{\Psi} = \tilde{Q}(\mathbf{\Psi})$$
(30)

Eventually, eq. (27) further reduces to:

$$\tilde{Q}(\mathbf{\Psi}) = \sum_{j} \lambda_{j} (\triangle \Psi_{j})^{2} \tag{31}$$

where the λ_j are the eigenvalues of the system.

The general idea is that, once the principal axes (which are determined by the eigenvectors) have been identified, along with their associated eigenvalues, it is straightforward to calculate the principal solution change due to a parameter perturbation using eq. (31), and to identify the directions of perturbation that will lead to the largest solution modification, as they are associated to the largest eigenvalues. Thus, important reactions can be identified as the *large* eigenvector elements associated with *significant* eigenvalues. For example, if reaction parameter k_i does not appear in any \ll significant enough \gg eigenvalue

group ², then this reaction parameter has no or little effect on the solution (as it can be seen from eq. (31)). The selection of those significant eigenvalues and large eigenvector elements is an important step, based mostly on experience, and in its original version, KINALC asks the user to provide dedicated thresholds (see Annex B). This selection procedure and its implementation inside the FORTRAN program is further discussed in section 5.2.

Useful kinetic information can also be gained from the existence of small eigenvalues, as is thoroughly presented in [50], for the identification of potential QSS species.

This analysis can be performed similarly on the ${\bf F}$ matrix of the rate-of-production sensitivities (section 3.2.1), where the objective function will be the overall variation in the net rate-of-production of chosen species i. However, this analysis is not performed on different time points, as the time dependence is implied through the time derivative of the concentration vector. Also, it is worth mentioning that a reaction shown to be important by the ${\bf F}$ matrix analysis may still prove to be unimportant in considerations based on the ${\bf S}$ matrix, due to a "memory effect" of the latter (see [46] for further explanations). ${\bf F}$ depends only on the reaction rates ${\bf k}$ and on the concentrations ${\bf c}$, and is therefore especially suitable for obtaining local information. For this reason, PCA is usually performed on the rate-of-production matrix when looking for a set of important reactions.

 $^{^{2}}$ An eigenvalue group of reactions is composed of those reactions associated with the highest eigenvector elements - according to a user defined threshold- of this eigenvalue.

3.3 From skeletal schemes to reduced schemes

3.3.1 Quasi Steady State Approximation (QSSA)

QSSA hypothesis and principle Complex systems such as Eq. (2) often have many disparities in the represented timescales, some of them being extremely short. Over the past 50 years, a common approximation has been made to consider the short characteristic time intermediate species in a stationary state, considerably simplifying the time resolution of the system.

Lu and Law [23] gave an accurate definition of a Quasi Steady State (QSS) species: $\ll A$ QSS typically features a fast destruction time scale, such that its small or moderate creation rate is quickly balanced by the self-depleting destruction rate, causing it to remain in low concentration after a transient period. The net production rate of the QSS species is therefore negligible compared with both the creation and the destruction rates, resulting in an algebraic equation for its concentration \gg . Using the formalism developed in section 2, this leads to:

$$\frac{\partial c_i}{\partial t} = f_i(\mathbf{c}, \mathbf{k}) \approx 0$$
, for QSS species i (32)

With this approximation, the (net) rate-of-production expressions for QSS species lead to a set of algebraic equations, functions of an arbitrary number of species concentration and an arbitrary number of reaction rates. Those expressions allow to eliminate QSS species from eq. (2), thus lowering the order of the nonlinear system of differential equations and reducing the chemical mechanism's stiffness. However, due to the Arrhenius formulation of the reaction rates, such algebraic equations are not linear, and they can quickly prove to be very complex for only a few number of assumed QSS species. *Truncation* is then needed to provide additional simplification, which consists in neglecting the concentration of those species only present in very small quantities, prior to implementation of the reduced kinetics.

Now, the QSSA allows the concentration of some species (the QSS species) to be calculated from the concentration of other species, via the algebraic set of Eq. (32), instead of from the set of differential Eq. (2). It is possible to estimate the difference in concentration of QSS species obtained via the two methods, at a chosen point along the trajectory of the kinetic system. This difference is referred to as the instantaneous QSSA error [48]. It is called QSSAS when evaluated for a single QSS species, or QSSAG when evaluated on a group of QSS species. The simplest method to calculate the errors of QSS species is to calculate both solutions with and without QSSA. However, this method is often inefficient, mainly due to computational time requirements. An alternative method is generally preferred, with great accuracy and limited calculation steps [48], which is explained in the next paragraph.

As this error propagates along the solution trajectory of the whole chemical system, it causes an overall error on the non-QSS species as well; but in practice, and if the QSS species are properly selected, this impact is considered insignificant in the time interval of calculation. This points out that a key question is the proper selection of the QSS species. KINALC offers criteria that depend on the tolerated levels of QSSAS and QSSAG errors to properly select the QSS species.

REMARK: It is eventually still the overall error on the important and necessary species that matters in the applicability of the QSSA. Usually, those species are non-QSS and thus, the evaluation of the instantaneous errors QSSAS and QSSAG is not sufficient. Furthermore, truncation can also be used as a mean to reduce the error on the concentration of the QSS species, as those are usually overestimated.

QSSA error estimation We will refer to the concentration vector calculated from Eq. (2) as \mathbf{c} ; whereas the concentration vector calculated from Eq. (2) with the QSSA of Eq. (32) on selected QSS species will be referred to as \mathbf{C} . The superscripts (1) and (2) refer to non-QSS species and QSS species respectively.

The QSSA-concentration vector is splitted in two: $\mathbf{C} = (\mathbf{C^{(1)}}, \mathbf{C^{(2)}})$, and assuming that the error on non-QSS species is negligeable, we have $\mathbf{C^{(1)}} \approx \mathbf{c^{(1)}}$, so that actually $\mathbf{C} \approx (\mathbf{c^{(1)}}, \mathbf{C^{(2)}})$.

For every QSS species i, a Taylor approximation of its rate-of-production $\partial c_i^{(2)}/\partial t$ around $\mathbf{C}^{(2)}$ is used.

Neglecting the higher order terms gives:

$$\frac{\partial c_i^{(2)}(\mathbf{c}, \mathbf{k})}{\partial t} = f_i(\mathbf{C}, \mathbf{k}) + \sum_{p \in QSS} \left(\frac{\partial f_i(\mathbf{c}, \mathbf{k})}{\partial c_p^{(2)}} \right)_{\mathbf{c} = \mathbf{C}} \triangle c_p^{(2)} + \sum_{p \in non - QSS} \left(\frac{\partial f_i(\mathbf{c}, \mathbf{k})}{\partial c_p^{(1)}} \right)_{\mathbf{c} = \mathbf{C}} \triangle c_p^{(1)}$$
(33)

where $\triangle c_p^{(i)} = (c_p^{(i)} - C_p^{(i)}).$

With the approximations made before, the first and last terms of Eq. (33) are equal to zero, thus leaving:

$$\frac{\partial c_i^{(2)}}{\partial t} = \sum_{p \in QSS} \left(\frac{\partial f_i(\mathbf{c}, \mathbf{k})}{\partial c_p} \right)_{\mathbf{c} = \mathbf{C}} \triangle c_p^{(2)}$$
(34)

With the use of the Jacobian, one finally finds the error on species i:

$$\triangle c_i^{(2)} = \frac{1}{\mathbf{J}_{ii}} \frac{\partial c_i^{(2)}}{\partial t} - \frac{1}{\mathbf{J}_{ii}} \sum_{p \in OSS \neq i} \mathbf{J}_{ip} \triangle c_p^{(2)}$$
(35)

The QSS error induced on a single species by that same species is often considered to be dominant, leading to the following approximation of Eq. (35) [48]:

$$\Delta c_i^{(2)} = \frac{1}{\mathbf{J}_{ii}} \frac{\partial c_i^{(2)}}{\partial t} \tag{36}$$

Eq. (36) implies that the rate-of-production of a QSS species (without QSSA) is not exactly 0, and that the Jacobian term (so, the sensitivity of the species to its own concentration) must be large enough for the QSSA to be sufficiently accurate.

In both QSSAS and QSSAG cases, the *fractional instantaneous error* is calculated from the instantaneous one by [48]:

$$e_i(\%) = \frac{\triangle c_i^{(2)}}{c_i^{(2)}} \times 100$$
 (37)

REMARK: Starting from eq. (33), the error $\triangle c_l$ on selected species is only an **approximation** of the real error that could be estimated from a difference in running the mechanism with and without QSSA!

The QSSAG error calculation is based on eq. (35), applied to a selected group of QSS species c_i , $i \in [QSS]$.

3.3.2 Time-scale analysis: Computational Singular Perturbation (CSP)

In conventional simplified kinetics modeling, the fast reactions and QSS species are identified based on a "try and error approach" and on intuition, and approximate analytical results are highly valued because of the insights they can provide when inspected by a theoretician. In many cases, QSS species are chemical radicals, but not always. Computational Singular Perturbation (CSP) theory is a tool that allows the selection of QSS species based on the analysis of *characteristic timescales*, by choosing to express the rate-of-production vectors differently from Eq. (2).

CSP expresses \mathbf{f} in Eq. (2) in an alternative representation system, and looks for basis vectors with special properties. Rate-of-production vectors are now *decomposed* along a set of basis vectors $\mathbf{v_d}$ called *directions* (of dimension n, the total number of chemical species).

$$\mathbf{f} = \sum_{0 < d < n} \mathbf{v_d} f^d \tag{38}$$

where the f^{d} 's are called the *amplitudes* of the chemical system, and reads:

$$f^d = \mathbf{w}^d \bullet \mathbf{f} \tag{39}$$

with $\mathbf{w}^{\mathbf{d}}$, $d \in [1, n]$ being the set of inverse row basis vectors:

$$\mathbf{w}^{\mathbf{d}} \bullet \mathbf{v}_{\mathbf{b}} = \delta^{d}_{b}, \quad d, b \in [1, n] \tag{40}$$

Each of the additive terms in Eq. 38 in this context is called a reaction mode. Here, basis vectors are defined to differentiate species according to whether their evolution is explosive, fast, slow or dormant. This analysis is carried out on the basis of an eigenvalue-eigenvector decomposition of the matrix \mathcal{M} linking the amplitudes f^d , to their derivative:

$$\frac{\partial f^d}{\partial t} = \sum_{0 < b < n} \mathcal{M}_b{}^d f^b \tag{41}$$

 \mathcal{M} depends on the local Jacobian, as well as on the new basis vectors (see [17], [25], or [8], for a more thorough description of the CSP method used by KINALC).

The idea is to find a set of directions that will uncouple the different amplitudes associated to them; i.e we try to have \mathcal{M} as diagonal as possible in Eq. (41). Eigenvalues reciprocals have time dimension and are subsequently referred to as timescale $(\tau(d))_{d \in [1,n]}$. Those timescales can be ranked from the smallest to the largest, thus providing a ranking of the amplitudes and of the reaction modes as well.

Once the proper decomposition of \mathbf{f} is found -and after refinement if necessary (see [17, 16])- the next step is to choose a cutting timescale $\tau(M)$ as being the smallest time length considered, and then to find out the decomposition of each species' rate-of-production according to the M fastest modes only -so, on a fast subspace:

$$\mathbf{f}_{fast} = \sum_{0 < d < M} \mathbf{v_d} f^d \tag{42}$$

Or, starting from the expression of \mathbf{f} provided by Eq. 2:

$$\mathbf{f}_{fast} = \left(\sum_{0 < d < M} \mathbf{Q}_d\right) \bullet \mathbf{f} \tag{43}$$

where the \mathbf{Q}_d , $d \in [1, M]$ are the set of fast projection matrices (of dimension $n \times n$):

$$\mathbf{Q}_d = \mathbf{v}_d \, \mathbf{w}^d \tag{44}$$

Furthermore, the diagonal elements of the fast projection matrices $\mathbf{Q}_d(i)$, $i \in [1, n]$ form a set of fast subspace radical pointer of the *i*-th species onto the *d*-th mode. According to [17], whenever the sum of the fast subspace pointers $\sum_{0 < d < M} \mathbf{Q}_d(i)$ is greater than a specified threshold ϵ , then the considered species *i* is well decomposed onto the fast subspace, and is thus a good QSS candidate. This criterion is used by KINALC.

4 Numerical tools

4.1 The CHEMKIN II package

4.1.1 General presentation

All the calculations and numerical simulations in this report have been performed with the CHEMKIN-II package [15], which is a set of programs and subroutine libraries written in FORTRAN 77 for the simulation of various academic combustion configurations. More specifically, the Perfectly Stirred Reactor (PSR) and PREMIX programs, aim at simulating the evolution of a chemical reaction in an adiabatic vessel and the free propagation of a one dimensional premixed flame, respectively.

To solve the equations governing the evolution of the chemical system, which are coded inside the sub-routine libraries called by the different programs, CHEMKIN-II needs thermodynamic and transport data:

- The thermodynamic database is mainly modeled from the JANAF tables (1971). It contains polynomial coefficients for the evaluation of the specific heat (C_p) and standard enthalpies (H^0) and entropies (S^0) , following the \ll NASA Chemical Equilibrium formalism \gg : for each species, two sets of seven polynomial coefficients are available, depending on the temperature range (resp. between 300 and 1000 K and 1000 and 5000 K). Those thermodynamic quantities (standard enthalpy and entropy) are further necessary in order to evaluate the j-th reaction's equilibrium constant K_{p_j} which allows the determination of the j-th inverse reaction coefficient k_{rj} , following the equations presented in section 3.1.
- The transport database contains molecular parameters for a large number of species, which are used to calculate transport properties when necessary (it is the case for the program PREMIX), such as thermal conductivity, viscosity, diffusion coefficients, and thermal diffusion coefficients.

Those data are interpreted by specific programs (or *interpreters*) to ultimately produce binary outputs (.link and .linktp) required by the programs to be used through a series of specific subroutines. Fig. (2) displays a schematic of CHEMKIN-II's architecture.

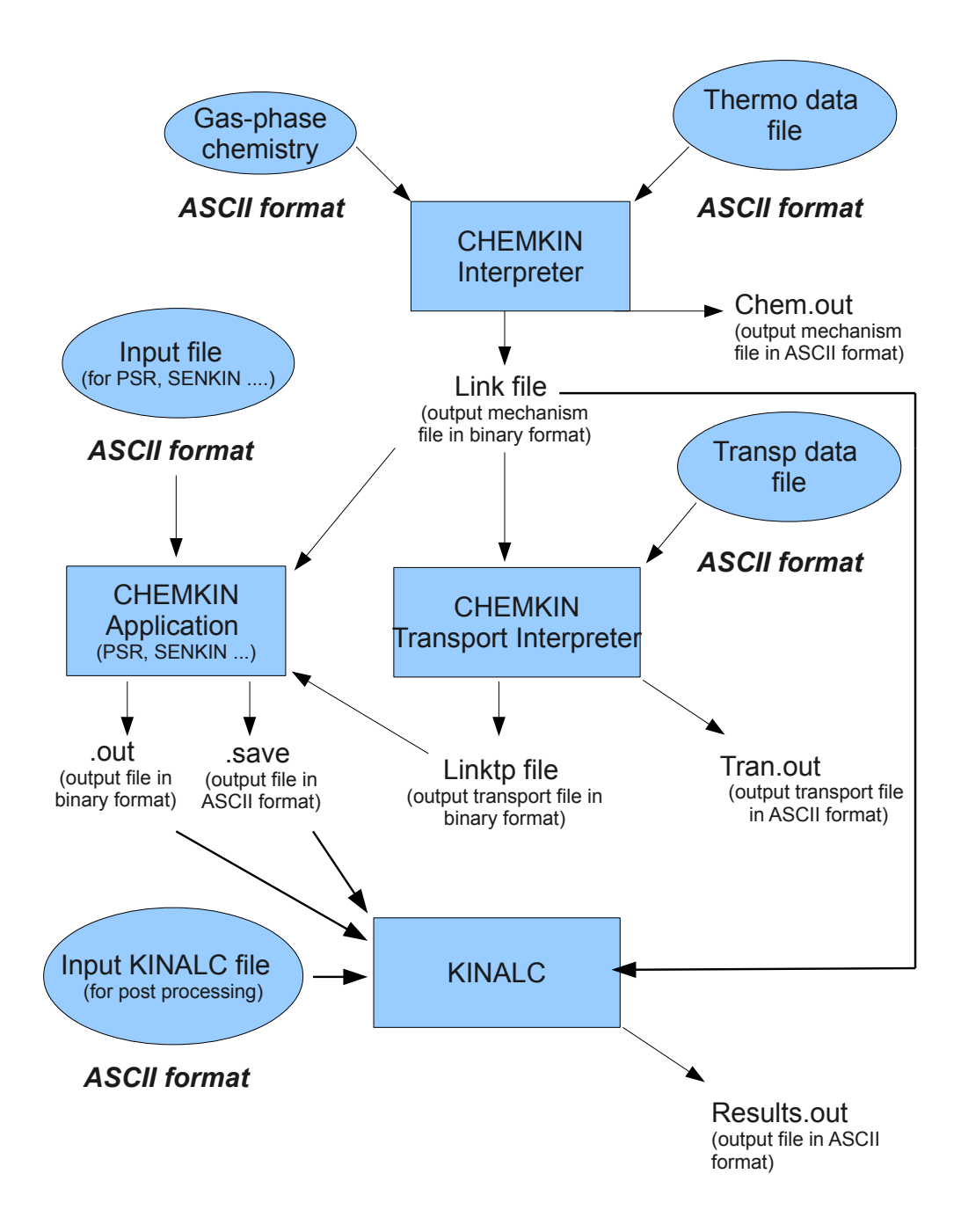


Figure 2: CHEMKIN-II structure and interaction with KINALC

4.1.2 Perfectly Stirred Reactor (PSR)

The PSR of Fig. (3) is characterized by its volume V, residence time τ and heat loss Q (assumed equal to zero in our case). The inlet temperature, mass flow rate (or density) and mixture composition of the gas should also be specified.

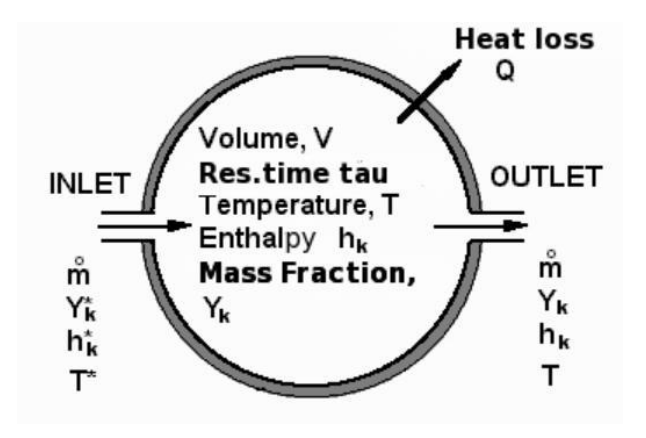


Figure 3: Schematic representation of a Perfectly Stirred Reactor

The PSR solves a set of non-linear algebraic equations to obtain the temporal evolution of the temperature and the mass fraction profile of all species inside the reactor, Y_i , $i \in [1, n]$. Though we look for the solution to the steady-state equations, the computational algorithm often requires a partial solution of the related transient problem, typically, whenever the resolution method fails to converge. Therefore, the transient conservation equations for the PSR are presented hereafter.

The time-dependent equation for mass conservation of each gas-phase species, ignoring the implicit time dependence of ρ through its dependence on the temperature and molecular weight, and all surface interaction, is ([32]):

$$\rho.V.\frac{dY_i}{dt} = -\dot{m}.(Y_i - Y_i^*) + f_i.W_i.V$$
(45)

or:

$$\frac{dY_i}{dt} = -\frac{1}{\tau} \cdot (Y_i - Y_i^*) + \frac{f_i \cdot W_i}{\rho}$$
(46)

where W_i is the molecular weight of the *i*-th species and f_i is the molar rate of production by gas-phase chemical reaction per unit volume. The superscript * indicates inlet stream quantities, as in Fig. (3). ρ is calculated through the equation of state:

$$\rho = \frac{P.\overline{W}}{RT} \tag{47}$$

where P is the static pressure, \overline{W} is the mean molecular weight of the mixture, R is the universal gas constant and T is the temperature.

The energy equation, under the same assumptions for ρ and neglecting the bulk, surface and wall contributions reads:

$$\rho.V.\frac{dh}{dt} = -\dot{m}.\sum_{0 < i < n} (Y_i h_i - Y_i^* h_i^*) - Q \tag{48}$$

or:

$$\frac{dh}{dt} = -\frac{1}{\tau} \cdot \sum_{0 < i < n} (Y_i h_i - Y_i^* h_i^*) - \frac{Q}{\rho \cdot V}$$
(49)

where h is the specific enthalpy of the gas mixture, equal to the sum of the product of the species mass fraction and the pure species specific enthalpy:

$$h = \sum_{0 < i < n} Y_i h_i \tag{50}$$

If the specific heat capacity is defined in the same way:

$$\overline{C_p} = \sum_{0 \le i \le n} Y_i C_{p_i} \tag{51}$$

where C_{p_i} is the heat capacity of the *i*-th species, then the derivative of Eq. (50) reads:

$$\frac{dh}{dt} = \overline{C_p} \frac{dT}{dt} + \sum_{0 < i < n} h_i \frac{dY_i}{dt}$$
(52)

By combining eq. (46), (49) and (52), the equation governing the temperature evolution can be derived:

$$\overline{C_p} \frac{dT}{dt} = \frac{1}{\tau} \cdot \sum_{0 < i < n} Y_i^* (h_i^* - h_i) - \sum_{0 < i < n} \left(\frac{h_i f_i W_i}{\rho} \right) - \frac{Q}{\rho V}$$
 (53)

The system of steady state equations (so, with the time derivative terms equal to 0) composed of eq.(46) and (53) is solved by a modified Newton method, whose details can be found in [32].

4.1.3 One dimensional propagating premixed flame (PREMIX)

The PREMIX program computes the species and temperature profiles in both steady-state burner-stabilized and freely propagating premixed adiabatic laminar flames. It accounts for finite rate chemical kinetics and multi-component molecular transport. In this report, only freely propagating premixed adiabatic flames have been simulated. The only difference lies in the boundary condition when solving for the governing equations. Indeed, in this case, the mass flow rate \dot{m} is an eigenvalue, and must be determined as part of the solution. Therefore, an additional boundary condition is required, and we fix the location of the flame by specifying the temperature at one point.

The equations governing steady, isobaric, quasi-one-dimensional flame propagation may be written as follows [14]:

$$\dot{m} = \rho.v.A = C \tag{54}$$

$$\dot{m}\frac{dY_i}{dx} + \frac{d}{dz}(\rho.A.Y_i.V_i) - A.f_i.W_i = 0; \quad i \in [1, n]$$
 (55)

$$\dot{m}\frac{dT}{dx} - \frac{1}{\overline{C_p}} \cdot \frac{d}{dx} \left(\lambda A \cdot \frac{dT}{dx} \right) + \frac{A}{\overline{C_p}} \cdot \sum_{0 < i < n} \rho Y_i V_i C_{p_i} \cdot \frac{dT}{dx} + \frac{A}{\overline{C_p}} \cdot \sum_{0 < i < n} f_i h_i W_i = 0$$
 (56)

where v denotes the velocity of the fluid mixture, A the cross-sectional area of the stream tube encompassing the flame which, by default, is taken to be constant and equal to unity; λ is the thermal conductivity of the mixture and x is the spatial coordinate.

The program also allows the user to choose how to evaluate the transport properties by either using mixture-averaged formulas or a multi-component diffusion model. With the more accurate multi-component option, the transport property evaluation follows the method described by Dixon-Lewis in [6]. The diffusion coefficients, thermal conductivities, and thermal diffusion coefficients are computed from the solution of a system of equations defined by a so-called L matrix, composed of nine block sub-matrices. The different transport terms are detailed in [13].

Here again, the system of governing differential equation is solved by a modified Newton method, whose

details can be found here [13].

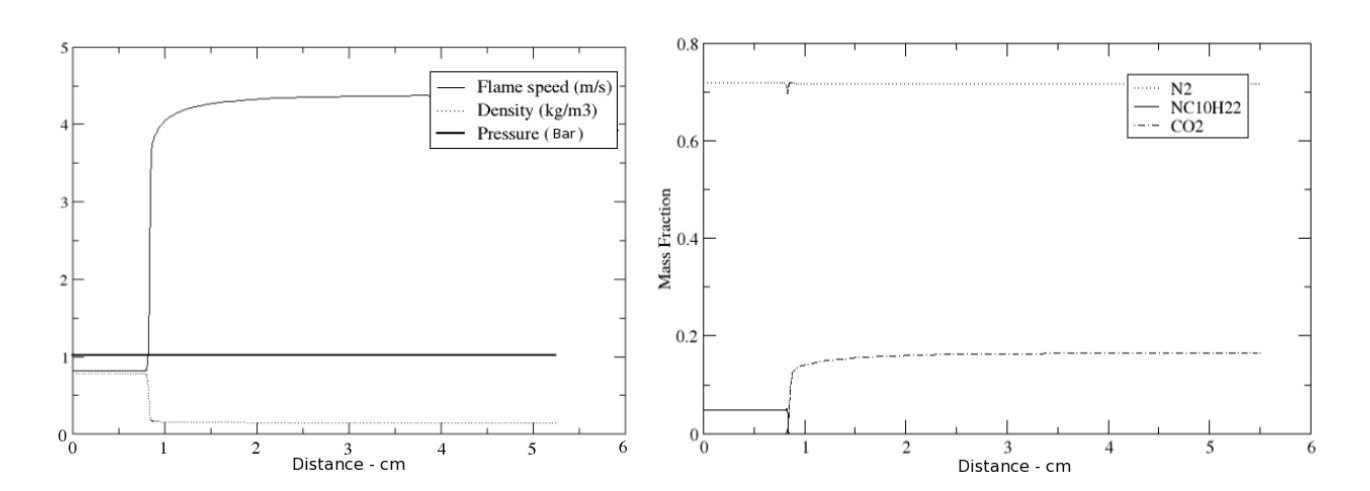


Figure 4: Example of graphs of PREMIX calculated quantities. Changes occur at the location of the flame front.

4.2 KINALC: A program for the kinetic analysis of reaction mechanisms

KINALC is an open source FORTRAN 77 program designed for the kinetic analysis of combustion reaction mechanisms. It was developed by researchers of the University of Leeds in the UK and the Etvs University (ELTE) in Budapest, and can be downloaded on from their internet website [47]. KINALC is a post-processor to the simulation programs of the CHEMKIN-II, III and IV package (SENKIN [28], PRE-MIX [14], OPPDIF, PSR, SHOCK, and EQLIB for CHEMKIN-II [15]; SENKIN, PREMIX, OPPDIF, SHOCK, and EQUIL for CHEMKIN-III; Closed Homogeneous, Equilibrium, Flame speed calculator, Incident Shock, Opposed flow flame, Perfectly Stirred Reactor, Pre-mixed burner, Reflected Shock model with CHEMKIN-IV), and can be used in order to derive skeletal and reduced schemes from detailed ones, with some of the most common analytical methods in use today in that field (and explained in section 3).

More specifically, KINALC carries out three types of analysis [49]:

- it processes concentration sensitivity analysis results
- it extracts information from reaction rates and stoichiometry
- it provides kinetic information about the species

KINALC processes the concentration sensitivity information in three different ways [49]: it can select the important pieces of information from the sensitivity results dumped by the simulation programs, calculate the sensitivity of objective functions for given species and carry out the mathematical principal component analysis on given matrices. Using information on reaction rates and stoichiometry it is able to produce a matrix of the sensitivity of reaction rates and analyze fluxes of elements from species to species to ultimately give a summary of important reactions. Finally, it provides kinetic information about the species by traditional rate-of-production analysis and investigation of the *Jacobian* to allow a reduction of the number of species and an estimation of the instantaneous error associated to Quasi Steady State (QSS) species. Ultimately, the information delivered by KINALC is useful for uncertainty analysis, parameter estimation, experimental design, and mechanism reduction [47].

KINALC has been designed to be very user friendly, and a lot of information about why and how it should be used can be found online [47], as well as inside the FORTRAN 77 file kinalc.f itself. However, the mathematical treatments applied are not always transparent and are sometimes redundant. For a more detailed description of available options and hidden performed calculations, refer to section 3. Two examples of use under CHEMKIN-II and the 3.18 sources can be found in section 5.

REMARK: Depending on the type of analysis performed, KINALC works on two different types of binary mechanism file (the .link, see Fig. (2)). Most of the time, it asks for a fully irreversible mechanism, which can be obtained from a reversible one (from the .link file) using FORTRAN program *Mechmod* (see online at http://garfield.chem.elte.hu/Combustion/mechmod.htm). Mechmod needs to be compiled with the dcklib.f subroutine of CHEMKIN-II package. Mechmod also reads thermodynamic data, converts the units and can remove selected species from a given mechanism.

5 Example of reductions with KINALC

5.1 The CSP option of KINALC applied to a Methane-Air skeletal scheme to identify QSS species

5.1.1 Skeletal scheme description and methodology

Skeletal scheme description: The analysis is carried on a 30 species skeletal scheme for Methane-Air oxidation developed by Lu [21], which served as the basis to derive reduced schemes for both auto ignition and extinction [24]. This mechanism contains 183 reversible reactions, which is still too large for efficient computational applications in combustion.

As demanded by KINALC, the skeletal mechanism is first transformed by the program *Mechmod* [47] into a scheme of irreversible reactions only. A preliminary job has then been carried out, where we have demonstrated the accuracy of the skeletal "Mechmod" mechanism through a series of auto-ignition, extinction and 1D calculations with CHEMKIN-II simulation programs (SENKIN [28], PSR and PREMIX). Indeed, when applying the Mechmod transform, a set of three temperatures must be chosen for the evaluation of the *equilibrium constants* (see section 3.1) used to establish the reverse reaction parameters. In principle, these temperatures should be taken at the peak activity of each reverse reaction, to best match the original mechanism results (where reverse reaction parameters are evaluated "on the fly"). However, it has been checked that the choice of 1000.0 K, 1750.0 K, and 2500.0 K finally done for the methane mechanism gives accurate results for all test cases (see Fig. (5)). The new mechanism now contains 359 irreversible reactions.

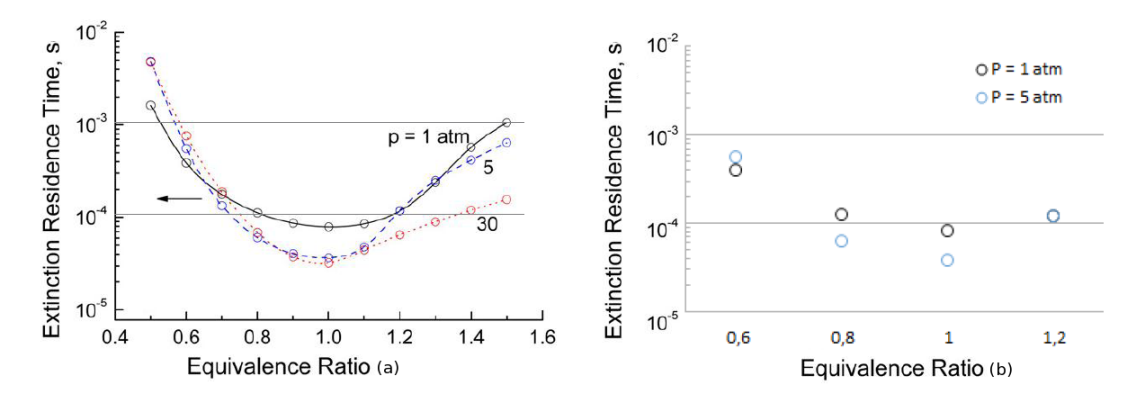


Figure 5: Extinction residence time of PSR as function of pressure and mixture equivalence ratio, calculated by Lu and Law with the detailed GRI 3.0 mechanism ((a) - dotted line from [24]) and calculated by CHEMKIN with the skeletal "Mechanism irreversible mechanism (b).

Methodology: Lu and Law [24] applied the CSP method (see paragraph 3.3.2) on auto ignition and extinction cases, respectively, to identify the candidate QSS species as being those with *fast* timescales τ_{fast} when compared to auto-ignition and extinction characteristic timescales τ_{char} , respectively:

$$\tau_{fast} < \frac{\tau_{char}}{\alpha} \tag{57}$$

where α is a safety factor set equal to 50.

Indeed, these are the shortest timescales for the major radical pool to build up, given a sufficiently high temperature and radical concentrations, such that the reactions can sustain themselves, and therefore the best possible candidates [22]. More specifically, QSS species are selected on the basis that their projection onto the fast subspace -characterized by the previous limit on the timescales τ_{char}/α (see paragraph 3.3.2), has to be greater than a specified threshold ϵ set here equal to 0.9.

The parameter range covered for the CSP analysis, respectively, by Lu and Law and in this report, is as follows:

	CSP Analysis with KINALC in this report	CSP Analysis in [24]
Equivalence ratios	0.6 - 1.2	0.5 - 1.5
Pressure range (atm)	1 - 5	1 - 30
Initial temperature values	1000 - 1800	1000 - 1600
(K) (SENKIN)		
Initial temperature values	300	300
(K) (PSR)		

Lu and Law eventually removed eleven species and associated reactions from their original 30 species skeletal mechanism, so that their final reduced mechanism only retained 19 species and 15 *global* steps. The procedure is reproduced here to verify the good usage of KINALC.

KINALC procedure: The steps to follow for a complete *standard reduction process* through a KI-NALC analysis of CHEMKIN simulations are (with the example of the PSR simulations program):

- Definition of the application range,
- Creation of the PSR inputs, and running a first set of PSR simulations to extract each τ_{ext} and analysis points,
- Personalization of the KINALC input file to each analysis point, and launch of a set of KINALC post processing,
- Analysis of each KINALC output file, to decide which species/reactions to dump/combine from the initial scheme,
- Writing of a new scheme,
- Validation of the new scheme

According to this, once the application range is defined (see last paragraph), the next step is the launch of the required simulations with the CHEMKIN-II simulations programs PSR and SENKIN, as is required for the CSP analysis with post-processor KINALC. See Fig. (6) for details regarding the configurations of the different simulations. The extinction time and temperature with PSR is obtained through a series of restart in all cases. Also, a first sensitivity analysis is carried out by CHEMKIN, as it is often required by KINALC.

Once a solution is obtained for all cases, the CSP analysis with post-processor KINALC is performed. Only one analysis point is chosen for each configuration (see Fig. (6)): for PSR simulation, the residence time is fixed and equal to 1 sec, while for SENKIN simulations the KINALC analysis time is taken in the ignition vicinity.

For this particular test, no modification of the KINALC fortran program was made, and the analysis is simply performed on each case by using the CSP keyword (see Annex B) in the KINALC input file, followed by the characteristic timescale divided by 50 -as we have seen that this is the limiting timescale. As explained in the previous paragraph, the characteristic timescale is taken to be the extinction time for all extinction simulations run with PSR as well as for the laminar 1D flame simulation run with PREMIX; and the auto ignition delay is used for all auto-ignition simulations run with SENKIN (see the upper table of Fig. (7)).

Finally, the QSS species are identified on the KINALC output file, as being those whose projection onto the fast subspace is greater than $\epsilon = 0.9$. See Fig. (8) for an example of KINALC output file.

	PSR			
P = 1 atm				
Phi	0.6	0.8	1	1.2
Te			-	
300 K	Tau : 1	Tau : 1	Tau : 1	Tau : 1
P = 5 atm				
Phi	0.6	0.8	1	1.2
Te	0.0	0.0		1.2
300 K	Tau : 1	Tau : 1	Tau : 1	Tau : 1
	SENKIN			
<u>P = 1 atm</u>			<u>P = 5 atm</u>	
Phi	1		Phi	1
Те			Te	
1000 K	Around		1000 K	Around
1000 K	ignition		1000 K	ignition
1050 K	Around ignition		1050 K	Around ignition
1000 16	Around		4000 14	Around
1200 K	ignition		1200 K	ignition
1400 K	Around ignition		1400 K	Around ignition
	Around			Around
1600 K	ignition		1600 K	ignition
1800 K	Around ignition		1800 K	Around ignition
				.9
	SENKIN			
	P = 1 atm			
	Phi	1		
	Te			
	Mass Flow Rate	0.0366 g/cm2-s	Analysis performed at low temperature	
	Nate	g/cmz-s	(<1300 K)	

Figure 6: Calculation performed with CHEMKIN-II simulation programs, on a skeletal Methane/Air oxidation mechanism developed by Lu and Law [21], and analysis points considered for the KINALC QSSA analysis.

5.1.2 Results and conclusion

In accordance with the results presented in the paper by Lu and Law [24], the eleven species C, CH, CH_2 , $CH_2(S)$, HCO, CH_2OH , CH_3O , C_2H_3 , C_2H_5 , HCCO and CH_2CHO have been eliminated by KINALC, for all extinction cases (PSR) as well as for the laminar 1D flame (PREMIX). The CSP by KINALC on the auto ignition cases (SENKIN), however, only returned the "good" QSS candidates for low temperature cases. A table of the QSS candidates found by KINALC on the extinction and laminar 1D cases is presented in the bottom table of Fig. (7).

It is interesting to see, when performing those type of post processing with KINALC, that the O and HCCO species seem to be the "least good QSS candidates", consistently with what Lu and Law commented on their paper. Indeed, the O species is already found to be a good QSS candidate for half of the cases (see Fig.(8)), and if the threshold ϵ on the CSP pointer is relaxed to 0.8 instead of 0.9, then it can be added to the list of QSS species for all cases (see Fig. (9)). However, it seems that it would \ll cause a relatively large increase in the reduction error for only a minor extent of reduction \gg [24]. On the other hand, if the threshold ϵ is increased, the HCCO species is not always identified as a good QSS species by KINALC (see Fig. (9)).

As can be seen from Fig. (7), (8) and (9), the H_2O_2 species appears to be a good QSS candidate. It is an assumption broadly used [22, 31]; however, it was not always found to be a good QSS candidate on the auto-ignition cases (SENKIN), consistently with what Lu and Law commented on their article [24], and with previous results [41].

It is worth noting also that, if in most cases, it is adequate to apply the reduced chemistry generated from PSR to laminar premixed flames because the chemical extinction time is expected to be shorter than the global diffusion time, the situation is different when dealing with auto ignition. Indeed, during auto ignition, species timescales as well as their concentration vary greatly, rendering quite difficult the selection of analysis points for the KINALC evaluation.

<u>PSR</u>									PREMIX	
	P = 1 atm T	e=300 K			P = 5 atm 7	Te=300 K				
Phi	0.6	0.8	1	1.2	0.6	0.8	1	1.2	P = 1 atm	
Extinction Res Time (s)	3.90E-004	1.20E-004	7.90E-005	1.18E-004	5.53E-004	6.05E-005	3.65E-005	1.18E-004	Temp (K)	1300
Chara. Time scale (s)	7.60E-006	2.20E-006	2.00E-006	2.30E-006	1.10E-005	1.21E-006	7.30E-007	2.30E-006	Chara. Time scale (s)	1.58E-06
Espèces (i)	Espèces QSS	Espèces (i)	Espèces QSS							
0	*			*				*	0	
Н	*	*			*	*			Н	
HO2		*	*	*	*	*	*	*	HO2	
H2O2	*	*	*	*	*	*	*	*	H2O2	
CH2O			*		*	*	*		CH2O	
СНЗ					*				CH3	
СНЗОН			*	*			*	*	СНЗОН	
C2H6			*	*	*	*	*	*	C2H6	
С	*/**	*/**	*/**	*/**	*/**	*/**	*/**	*/**	С	*/**
СН	*/**	*/**	*/**	*/**	*/**	*/**	*/**	*/**	СН	*/**
CH2	*/**	*/**	*/**	*/**	*/**	*/**	*/**	*/**	CH2	*/**
CH2(S)	*/**	*/**	*/**	*/**	*/**	*/**	*/**	*/**	CH2(S)	*/**
нсо	*/**	*/**	*/**	*/**	*/**	*/**	*/**	*/**	нсо	*/**
СН2ОН	*/**	*/**	*/**	*/**	*/**	*/**	*/**	*/**	СН2ОН	*/**
СНЗО	*/**	*/**	*/**	*/**	*/**	*/**	*/**	*/**	СНЗО	*/**
C2H3	*/**	*/**	*/**	*/**	*/**	*/**	*/**	*/**	C2H3	*/**
C2H5	*/**	*/**	*/**	*/**	*/**	*/**	*/**	*/**	C2H5	*/**
нссо	*/**	*/**	*/**	*/**	*/**	*/**	*/**	*/**	нссо	*/**
СН2СНО	*/**	*/**	*/**	*/**	*/**	*/**	*/**	*/**	CH2CHO	*/**

Page 1

Figure 7: QSS species identified by the post processing of extinction cases (PSR) and laminar 1D free propagating flame (PREMIX) with KINALC (*), compared to QSS species identified by [24] (**).

* Mode 14	(Eigenva	alue: -2.3	37079E+05)
		"Fast" s	pecies
	Single mode		Cumulative
0	(0.883)	С	(1.000)
H20	(0.569)	CH	(1.000)
OH	(-0.461)	C2H3	(1.000)
C02	(0.056)	CH20H	(1.000)
CO	(-0.052)	CH30	(1.000)
Н	(0.029)	C2H5	(1.000)
CH3	(0.025)	CH2(S)	(1.000)
CH20	(-0.021)	HC0	(1.000)
H2	(-0.018)	HCC0	(1.000)
CH4	(-0.008)	CH2	(0.999)
H02	(-0.001)	H202	(0.992)
02	(-0.001)	Н	(0.967)
H202	(-0.000)	CH2CH0	(1.036)
HC0	(-0.000)	0	(0.926)
СН30Н	(-0.000)	H20	(0.564)
CH2	(-0.000)	C02	(0.034)
C2H2	(0.000)	CH3	(0.026)
C2H6	(-0.000)	H02	(0.009)
CH2(S)	(-0.000)	C2H6	(0.000)
CH30	(-0.000)	C2H4	(0.000)
C2H4	(0.000)	C2H2	(0.000)
CH2C0	(-0.000)	N2	(-0.000)
HCC0	(0.000)	CH30H	(-0.000)
CH20H	(0.000)	H2	(-0.004)
CH	(-0.000)	CH4	(-0.008)
C2H3	(-0.000)	02	(-0.013)
C2H5	(-0.000)	CH20	(-0.021)
CH2CH0	(0.000)	CO	(-0.030)
^^^^^	^^^^ FAST TIMES	CALES ^^^	^^^^^

*	Mode	15	(E	igenva	lue: -1.8	B2030E	+05)	
			Single mo	ode		Cur	nulativ	/e
	H02		(0.986)	C	(1.000)
	H20	2	(0.008)	CH	(1.000)
	0		(0.004)	C2H3	(1.000)
	Н		(0.002)	CH20H	(1.000)
	CH2	0	(0.001)	CH30	(1.000)
	02		(-0.001)	C2H5	(1.000)
	H20		(-0.001)	CH2(S)	(1.000)
	CH3		(0.001)	HC0	(1.000)
	C02		(0.000)	HCC0	(1.000)
	CO		(-0.000)	H202	(0.999)
	OH		(0.000)	CH2	(0.999)
	H2		(0.000)	H02	(0.995)
	CH4		(-0.000)	Н	(0.969)
	HC0		(-0.000)	CH2CH0	(1.036)
	CH3	0H	(-0.000)	0	(0.930)
	CH3	0	(-0.000)	H20	(0.564)
	CH2		(0.000)	C02	(0.035)
	CH2	0H	(0.000)	CH3	(0.027)
	CH2	(S)	(0.000)	C2H6	(0.000)
	C2H	2	(0.000)	C2H4	(0.000)
	C2H	6	(-0.000)	C2H2	(0.000)
	C2H	4	(0.000)	N2	(-	0.000)
	CH		(0.000)	CH30H	(-	0.000)
	CH2	C0	(-0.000)	H2	(-	0.004)
	C2H	5	(-0.000)	CH4	(-	-0.008)
	HCC		(0.000)	02	(-	0.015)
	C2H		(-0.000)	CH20		0.020)
	CH2	CH0	(0.000)	C0		0.030)
	C		(0.000)	CH2C0		0.035)
	N2		(0.000)	OH	(-	0.441)

Figure 8: Example of KINALC output file for the identification of "fast" species with the CSP option. PSR post-processing : $\Phi=0.6,\, P=1$ atm, $T_e=300$ K.

Mode 18		acue/.	17819E+05)
	Single mode		Cumulative
HCC0	(0.937)	HC0	(1.000)
CH2C0	(0.063)	C2H6	(1.000)
CH3	(0.000)	С	(1.000)
C2H2	(0.000)	CH2CH0	(1.000)
CH4	(0.000)	H202	(1.000)
СНЗОН	(0.000)	CH20	(1.000)
CH	(0.000)	C2H5	(1.000)
C2H4	(0.000)	CH30	(1.000)
CH20	(0.000)	CH20H	(1.000)
CH2CH0	,,	H02	(1.000)
C2H3	(-0.000)	CH	(1.000)
CH2(S)	(0.00 <u>0</u>	ic tho	(
C2H5	(-0.0)HCCO	ร แเย "จอส" คร	C spesies)
C2H6	(-0.0(<u>"least (</u>		
CH20H	(0.000)	CH2	(0.958)
CH30	(0.000)	HCC0	(0.937)
H2	(0.000)	Н	(0.827)
C0	(0.000)	0	(0.803)
0	(-0 000)	7 04	(0.298)
Н	O pointer is	2	(0.070)
CH2	"almost"	12C0	(0.063)
OH	high enough	13	(0.049)
02	(0.000)	H20	(0.002)
C	(-0.000)	C2H4	(0.001)
HC0	(0.000)	CH4	(0.000)
H02	(-0.000)	02	(0.000)
H20	(0.000)	CO	(0.000)
H202	(-0.000)	C2H2	(0.000)
C02	(0.000)	C02	(0.000)
N2	(-0.000)	N2	(0.000)
^^^^	-^^^^ FAST TIMES	CALES ^^^	^^^^^

Figure 9: Example of KINALC output file for the identification of "fast" species with the CSP option. PSR post-processing: $\Phi = 1$, P = 1 atm, $T_e = 300$ K.

vvvvvvvvvvvvvv SLOW TIMESCALES vvvvvvvvvvvvvvvvvvvv

5.2 A modified KINALC PCAF option applied to a Kerosene-Air skeletal scheme to identify redundant reactions

5.2.1 Skeletal scheme description

The skeletal schemes for the Kerosene presented and derived in this report are all based on a detailed Kerosene scheme developed by Dagaut [5] and actualized by Voisin [53], which is composed of 225 species and 1800 reversible elementary reactions (or 3493 irreversible reactions). As Kerosene is a complex mixture, it is based on a juxtaposition of previously developed detailed mechanisms for the 3 main reactant types usually present; namely, n-decane for the linear alkane part, n-propylbenzene for the aromatic part and n-propylcyclohexane for the naphtenic part. Amongst the 3493 irreversible reactions, 36 are pressure dependent ("fall-off"), and their reaction rate follow the *Lindemann* formalism [12, 20]. The determination of the formulation's constants is based on an orthogonal distance regression rather than on a least squares fitting, and is described in [27].

As this mechanism is too complex to be used as such, Luche in [27] derived a series of skeletal mechanisms of different sizes, with the help of KINALC. His goal was to obtain the smallest possible mechanism that would still reproduce correctly the main species profiles (with a relative error < 10%) while drastically reducing the required calculation time. To do so, the analysis is based on three *criteria*:

• %P, the predictivity of the mechanism Over the P parametric configurations, and for the n species of the mechanism, this quantity evaluates how many amongst those species i whose molar fraction X_i is > 20 ppm are represented with an error $err_i = \frac{\triangle X_i}{X_i} < 10\%$:

$$\%P = \frac{\sum_{p} \sum_{i} \chi_{p,i}(X_{p,i} \ge 10ppm, err_{p,i} \le 10\%)}{\sum_{p} \sum_{i} \chi_{p,i}(X_{p,i} \ge 10ppm)}$$
(58)

where $\chi_{p,i} = 1$ if for the condition p the species i satisfies what is inside the parenthesis.

• GC_{moy} , a calculation time comparison This quantity is only an arithmetic average, over the parametric range, of the comparison between the calculation time required when performing a simulation with a reduced mechanism (t_{red}) and the calculation time required when performing that same simulation with the detailed mechanism (t_{det}) :

$$GC_{moy} = \frac{\sum_{P} \frac{t_{det}}{t_{red}}}{P} \tag{59}$$

• E_r , a global criterion This quantity is used as the ultimate criterion:

$$E_r = \%P \times GC_{moy} \tag{60}$$

To match the goal of an efficient reduction, all those criteria need to be maximized.

He performed a first reduction based on a Path Flux analysis with different flux thresholds (see Table 2). The flux threshold defines a lower limit on the normalized incoming and outgoing total fluxes of each species (as defined in Eqs. (24) and (25) of section 3.2.2): those with smaller fluxes are removed from the initial mechanism. So, when the flux threshold increases, the mechanisms become smaller as more and more species are discarded. The flux threshold is higher in the case of the N element, as it has been verified that this reduction gave satisfactory results [27]. Next, from this first set of skeletal mechanisms, and based on his set of criteria, he chose to perform a second reduction based on a PCAF analysis (see Table 3) on two selected skeletal mechanisms: the one with C, H, O fluxes = 15, N fluxes = 25 (labeled 15/25) and the one with C, H, O fluxes = 15, N fluxes = 30 (labeled 15/30). The Flux in the case of the PCAF analysis refers to the threshold on the eigenvector elements associated with the largest eigenvalues (to obtain the significant eigenvalue groups, as defined in section 3.2.4): it allows to remove selected reactions, based on a methodology that will be discussed in details in the next paragraphs.

The resulting mechanisms are presented in table 2 and 3 hereafter.

Flux Thre	shold	Me	Mechanisms performance			bers
flux CHO	flux CHO flux N		%P	Er	species	Reactions
10	20	2.9	84.5	2.40	109	1644
10	25	3.0	84.2	2.50	107	1622
10	30	2.9	84.2	2.48	106	1616
10	35	3.1	84.1	2.5	105	1598
10	40	3.0	84.2	2.55	105	1598
15	20	3.7	79.6	2.97	93	1350
15	25	3.8	79.5	3.05	91	1328
15	30	4.0	79.5	3.15	89	1304
15	35	4.0	79.5	3.15	89	1304
15	40	4.0	79.5	3.15	89	1304
20	20	4.2	63.2	2.63	80	1060
20	25	4.2	63.8	2.66	78	1038
20	30	4.5	63.8	2.88	77	1032
20	35	4.3	63.8	2.74	76	1014
20	40	4.4	63.8	2.80	76	1014
	Initial	225	3493			

Table 2: Skeletal mechanisms derived by Luche [27] from a detailed Kerosene mechanism [5], by a Flux analysis on C, H, O and N elements. Highlighted mechanisms present the highest value of the global E_r criterion. From [27].

	Skel	etal		nanism 15 pecies)	5/25	Skeletal Mechanism 15/30 (89 species)				
	GC moy	%P	Er	Reactions	Red. factor	GC moy	%P	Er	Reactions	Red. factor
	mécanisi	ne dét	taillé	3493	-	mécanis	me dé	taillé	3493	-
Flux	3,8	79,5	3,05	1328	62,0%	4,0	79,5	3,15	1304	62,7%
1,000	4,92	79,3	3,90	991	71,6%	5,12	79,2	4,06	982	71,9%
0,995	6,55	78,8	5,16	748	78,6%	6,61	78,4	5,19	738	78,9%
0,990	6,66	78,6	5,23	713	79,6%	7,12	78,9	5,62	703	79,9%
0,985	7,20	78,5	5,65	694	80,1%	7,32	78,8	5,76	680	80,5%
0,980	7,05	78,8	5,56	680	80,5%	7,11	77,6	5,52	664	81,0%
0,975	7,19	77,6	5,58	670	80,8%	7,32	77,5	5,67	654	81,3%
0,970	7,29	75,8	5,53	657	81,2%	7,46	76,9	5,74	645	81,5%
0,965	7,29	76,5	5,57	650	81,4%	7,33	76,8	5,63	637	81,8%
0,960	7,31	76,0	5,56	642	81,6%	7,74	76,7	5,93	632	81,9%
0,955	7,31	76,3	5,58	634	81,8%	7,15	77,4	5,53	623	82,2%
0,950	7,53	78,5	5,91	625	82,1%	7,38	77,8	5,74	613	82,5%

Table 3: Skeletal mechanisms derived by Luche [27] from a detailed Kerosene mechanism [5], by a PCAF analysis performed on two prior skeletal mechanisms (15/25 and 15/30). Highlighted mechanisms present the highest value of the global E_r criterion. From [27].

Based on the results, the skeletal schemes used in this report are derived from the 15/25 and 15/30 skeletal mechanisms. More specifically, the modified PCAF analysis conducted next will be based on:

- First the 15/25 skeletal mechanism with a PCAF Flux equal to 1 (15/25 PCAF Flux = 1 in Table 3). It contains 991 reactions and 91 species (this mechanism will be referred to as the 15/25 PCAF 1 in what follows).
- Second the 15/30 skeletal mechanism with a PCAF Flux equal to 0.985 (15/30 PCAF Flux = 0.985 in Table 3). It contains 633 reactions and 89 species (this mechanism will be referred to as the 15/30 PCAF 0.985 in what follows).

It is worth noting here, that if results presented in [27] are correctly reproduced, it would confirm a posteriori the fact that the same reduction can be performed, either:

- Starting from an initial detailed mechanism, as it is almost always the case in the literature
- Or starting from any subsequently deduced skeletal scheme -provided that the reductions are all compatible and performed in a certain logical order.

5.2.2 Discussion about the methodology

The goal of this work was, here again, to verify the good usage of KINALC, but also to optimize its implementation; especially when the number of cases to run and post process starts to increase. Indeed, despite the fact that the previous analysis carried on the Methane-Air skeletal mechanism only required to run and post-process a dozen of PSR, SENKIN and PREMIX cases, it took over two weeks to finish everything. To understand why, one needs to remember the different steps to follow for a complete standard reduction process with KINALC, which was exposed in details in the previous section (5.1.1, KINALC procedure). Now, the time consumption of each of those steps is best put in light when considering that:

- CHEMKIN, in its provided version, is not set to run several different cases "in a row",
- KINALC, in its provided version, is not set to analyze several CHEMKIN outputs "in a row",
- CHEMKIN's input file, needs to be specific to each run cases,
- KINALC's input file, needs to be specific to each post-processed cases

To those reasons, we can now add the specificity of the PCAF option for the Kerosene-Air skeletal scheme analysis, which requires:

- To identify the necessary reactions from a series of KINALC post-processing, which is next to impossible without developing a dedicated code
- To remove unnecessary reactions from the scheme, which can be extremely daunting
- And to *compare* a newly KINALC reduced skeletal scheme to preexisting ones, to see "at a glance" which reactions have been eliminated

In order to ultimately being able to compare the potential new skeletal scheme to the detailed one in terms of predictivity and calculation time, by running a new set of PSR and PREMIX simulations. Finally, the number of analysis points in this report exceeds 60.

5.2.3 Semi-Automated PCAF procedure

In light of these considerations, it seems necessary to automatize parts of the reduction process, so as to avoid a long and tedious work which would inevitably lead to human errors. A preliminary job has then been carried out, where the post-processing main steps have been identified and personalized to a PCAF analysis, in order to focus on their automation (see the standard reduction process in section 5.1.1, KINALC procedure).

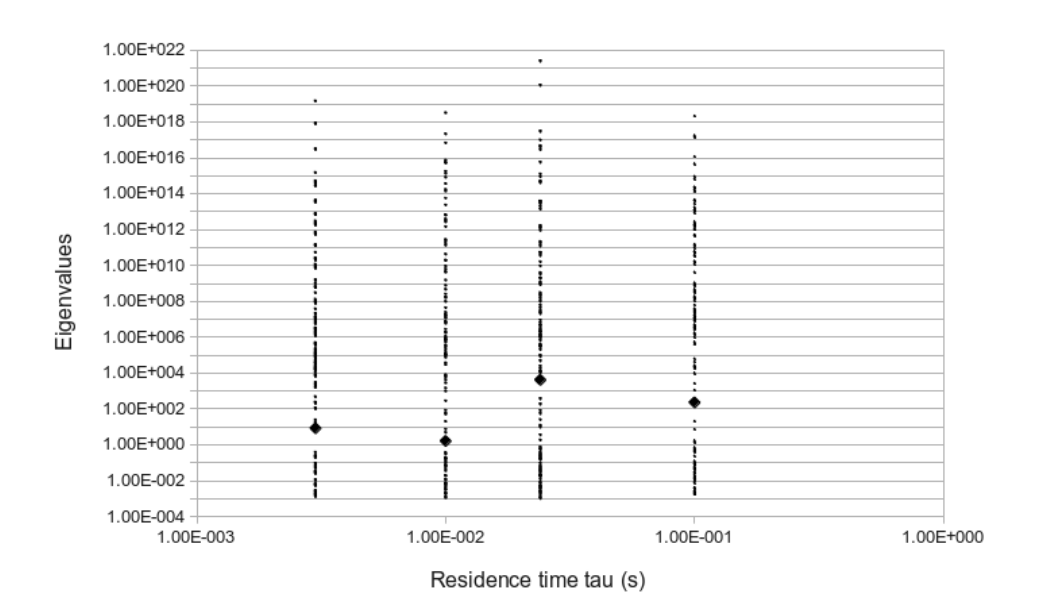


Figure 10: Example of eigenvalues repartition in function of the residence time, for a Methane-Air PSR simulation ($\phi = 1$, T = 300K, P = 1 atm). The biggest dots locate the gaps.

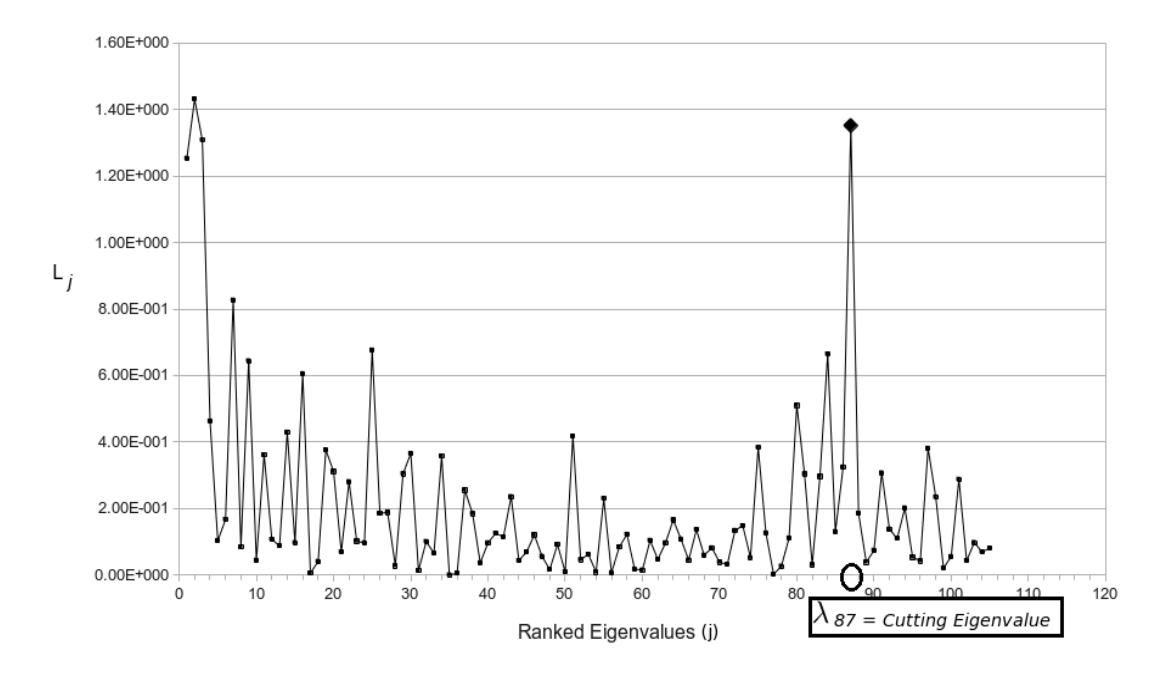


Figure 11: Example of cutting eigenvalue detection, for a Methane-Air PSR simulation ($\tau = 3.0 \cdot 10^{-3}$, $\phi = 1$, T = 300K, P = 1 atm)

In doing so, particular attention has been drawn to the personalization of the KINALC input file, where, in the PCAF analysis case, important reactions are selected on the basis of an eigenvalue threshold and an eigenvector threshold (see 3.2.4 for details regarding the PCAF analysis). Indeed, as it has been pointed out in recent work [18], it is best to try and adapt the eigenvalue threshold to each analysis point based on the repartition of its eigenvalues, than to choose a fixed threshold. This leads to the consideration of two new main steps, since in that case, two PCAF analysis with KINALC are required, followed by two analysis of the KINALC outputs. Fig. (17) in Annex C illustrates the final global post-processing scheme. The determination process of the eigenvalue threshold is described next.

When plotting the eigenvalues' repartition in function of the residence time, a jump can be detected, which can be used to set the eigenvalue threshold (illustrated on a Methane/Air skeletal scheme application, to allow better visualization, in Fig. (10)). A dedicated python code has been designed (CuttingLambda.py in Fig. (17)), whose goal is to automatically detect this jump, based on a first series of KINALC post processing run on all analysis points with a standard input file (Kinalc.sh in Fig. (17)). This code evaluates, for all cases, the difference L_j between the logarithm of two subsequent eigenvalues λ_j , λ_{j+1} , and looks for the largest one amongst a broad range of values (see Fig. (11)):

$$L_j = log(\lambda_j) - log(\lambda_{j+1}) \tag{61}$$

Another dedicated python code (KinalcInputWritter.py in Fig. (17)) will then rewrite the KINALC input file of all cases, so that another complete PCAF analysis with KINALC can be performed right away (Kinalc2.sh in Fig. (17)).

The python and shell codes used in the semi-automated procedure can be found in the adresses given in Annex C.

5.2.4 Modified PCAF option of KINALC, for the detection of important eigenvectors

As mentioned in section 3.2.4, each eigenvalue has an associated eigenvector, whose components u_j are each associated with a specific reaction j. As such, each eigenvalue, through its eigenvector, defines a reaction group. Now, once the largest eigenvalues have been detected, the next step is to identify the largest associated eigenvector components, so as to identify the important reaction groups, and eventually deduce the final set of important reactions (see Fig. 12).

To do so, for each eigenvalue, KINALC ranks eigenvector components and select the largest amongst

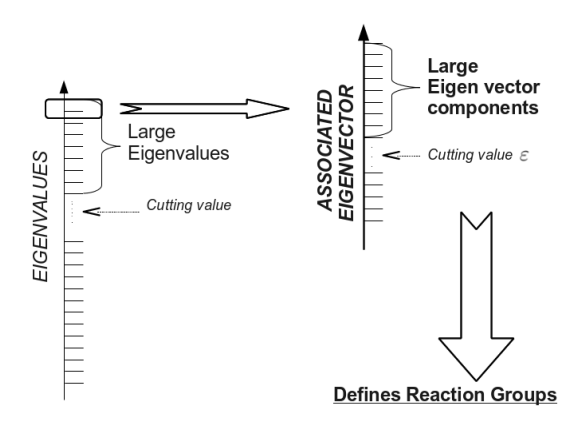


Figure 12: The reaction groups as defined by the PCA method

them, with respect to a dedicated threshold on their absolute values. To compare results with [27], this procedure has been altered: as all eigenvectors are normed, we sum the squares of the ranked components

 u_i on which we fix a maximum threshold $\varepsilon < 1$:

$$\sum_{1 < j < k} (u_j)^2 \le \varepsilon \tag{62}$$

Reactions associated with components k such that the sum of Eq. (62) is greater than ε are discarded.

5.2.5 Results and discussion

Skeletal scheme derivation: The parameter range for the PCAF analysis performed is as follows:

	PCAF Analysis with KINALC in this report	PCAF Analysis with KINALC in [27]
Equivalence ratio	0.5 - 2	0.5 - 2
Pressure	1 - 10	1 - 10
Inlet temperature	300 - 1200	300 - 1800

Since the parameter range in this report is smaller and included in the one used by Luche, the final skeletal mechanism deduced from a particular PCAF analysis with KINALC should theoretically be smaller than the one deduced from the same PCAF analysis in [27], and all the kept reactions at this step should also have been kept in [27] ³. To confirm this, the chosen eigenvector thresholds for the PCAF analysis (the Flux) based on the 15/25 PCAF 1 mechanism and 15/30 PCAF 0.985 mechanism were set to, respectively, 0.950 and 0.960; as these mechanisms have been derived in [27] and details about them are readily available (see Table 3).

See Fig. (13) for details regarding the configurations of the different simulations.

The results are in accordance with what was expected. Mechanisms deduced from the KINALC modified PCAF analysis now contain:

- 91 species and 493 reactions (15/25 PCAF 0.950), all of which are also part of the 625 reactions that form the skeletal 15/25 PCAF 0.950 scheme in [27] (see table 3), except for one reaction,
- 89 species and 494 reactions (15/30 PCAF 0.960), all of which are also part of the 633 reactions that form the skeletal 15/25 PCAF 0.960 scheme in [27] (see table 3), except for one reaction

There is one exception, in that both KINALC PCAF analysis suggested to keep the reaction $C_4H_2 + H(+M) => NC_4H_3(+M)$, whereas it was neglected in [27]. This reaction is of the termination type, and is usually required "far" from the extinction limit ($\tau >> \tau_{ext}$). Furthermore, it is always associated with one of the smallest eigenvalues, which makes it a "borderline" species and could have been neglected for chemical reasons even though KINALC suggested to keep it. However, for consistency, it has been kept in this work.

³Indeed, as it has been previously highlighted, the procedure in this work follows exactly the one from [18] and [27].

	P = 1 atm		
Phi	0.5	1	2
Te			
300	Tau2 : 1.00E-2 Tau3 : 2.40E-2	Tau1 : 9.00E-5 Tau2 : 2.00E-4 Tau3 : 2.00E-3 Tau4 : 2.00E-2 Tau5 : 1.00E-1	Tau2 : 1.00E-2 Tau3 : 4.00E-2
600	Tau2 : 4.00E-3 Tau3 : 2.00E-2	Tau1: 5.00E-5 Tau2: 1.00E-4 Tau3: 1.00E-3 Tau4: 1.00E-2 Tau5: 1.00E-1	Tau2 : 2.00E-3 Tau3 : 2.00E-2
900	Tau2 : 2.00E-3 Tau3 : 2.00E-2	Tau1 : 4.00E-4 Tau2 : 2.00E-3 Tau3 : 2.00E-2 Tau4 : 1.00E-1	Tau2 : 4.00E-3 Tau3 : 2.00E-2
1200	Tau2 : 2.00E-4 Tau3 : 2.00E-3	Tau1 : 2.00E-5 Tau2 : 2.00E-4 Tau3 : 2.00E-3 Tau4 : 4.00E-2	Tau2 : 2.00E-3 Tau3 : 2.00E-2

<u>P = 10 atm</u>					
Phi	1	1	2		
Te					
300		Tau1 : 4.00E-5 Tau2 : 4.00E-4 Tau3 : 6.00E-3 Tau4 : 6.00E-2			
600		Tau1 : 8.00E-5 Tau2 : 1.00E-3 Tau3 : 8.00E-3 Tau4 : 1.00E-1			
900					
1200		Tau1 : 2.00E-5 Tau2 : 2.00E-4 Tau3 : 4.00E-3 Tau4 : 1.00E-1			

	P = 3 atm		
Phi	0.5	1	2
Te			
300	Tau2 : 2.00E-2 Tau3 : 5.00E-2	Tau1 : 4.00E-4 Tau2 : 2.00E-3 Tau3 : 2.00E-2 Tau4 : 1.00E-1	Tau2 : 9.00E-3 Tau3 : 2.00E-2
600	Tau2 : 4.00E-3 Tau3 : 2.00E-2	Tau1 : 2.00E-4 Tau2 : 2.00E-3 Tau3 : 2.00E-2 Tau4 : 5.00E-1	Tau2 : 4.00E-3 Tau3 : 2.00E-2
900	Tau2 : 4.00E-4 Tau3 : 4.00E-3	Tau1 : 2.00E-5 Tau2 : 4.00E-4 Tau3 : 4.00E-3 Tau4 : 4.00E-2	Tau2 : 1.00E-3 Tau3 : 1.00E-2
1200			

Figure 13: Calculation performed with CHEMKIN-II PSR, on different skeletal Kerosene/Air oxidation mechanisms developed by Dagaut [5] and Luche [27], and analysis points considered for the KINALC PCAF analysis.

Skeletal scheme validation: To conclude, in order to be consistent with the objectives of a scheme reduction, we decided to validate the derived skeletal scheme on the parameter range of interest, as well as on a few added cases, with PSR simulations (see results in Annex D). A simulation of a one dimensional free propagating flame on an academic configuration (see results in Annex E) is also performed. The monitored quantities are:

- The extinction temperature and extinction time (PSR validation only)
- The flame speed (PREMIX validation only)
- The temperature profile
- The different fuels' mass fraction evolution (which are part of the *important* species)
- The main products mass fraction evolution
- The mass fraction evolution of radicals H, O and OH, which are also amongst the important species

Results pertaining to the 15/25 PCAF 0.950 scheme (labeled PCAF mec.) are the only ones presented and commented, since it turned out that this mechanism has both less reactions and a better predictivity than the 15/30 PCAF 0.960 scheme. The results are confronted with that of the detailed mechanism of [5] (labeled Detailed mec.) and, when relevant, of the 15/25 PCAF 1 mechanism in [27] (labeled Path Flux mec.), from which it is derived.

PSR Validation: On the parameter range of interest, the temperature profile as well as the extinction temperature are very well reproduced, with errors never exceeding 5% and rarely over 3%. The extinction time however, is usually underestimated, with errors well over 10% when not at stoichiometry. However, as can be seen on the tables at the end of Annex D, it is not clear whether the source of predictivity loss can be directly imputed to the PCA reduction, as the same error margins are often detected when comparing the Detailed mechanism to the Path Flux mechanism. It only seems that the extinction time predicted by the PCAF mechanism is very off in rich configurations.

In the same fashion, it appears that the predictivity of the Path Flux and PCAF mechanisms are about the same concerning the n-propylcyclohexane molar fraction profile (see Fig. (14)).

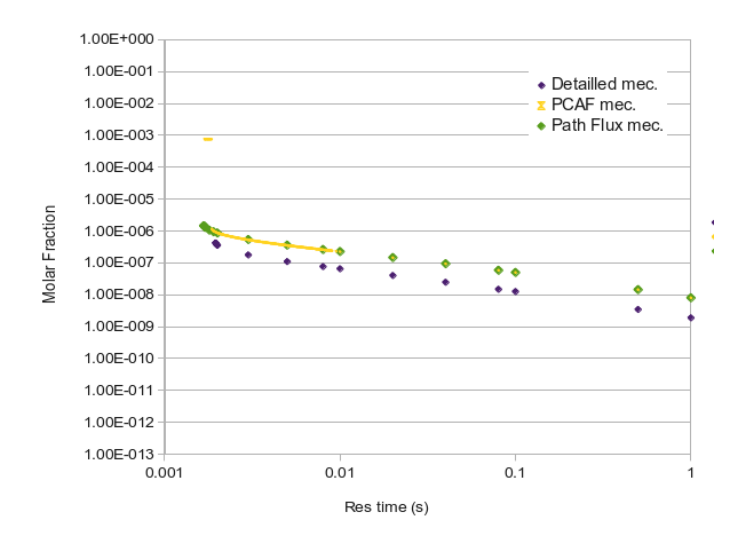


Figure 14: n-Propylcyclohexane molar fraction comparison between skeletal mechanisms ($\phi = 0.5, T = 300K, P = 1 \text{ atm}$)

Globally, the other fuels mass fraction evolution are well reproduced. The mechanism tends to slightly over estimate the fuels and radicals mass fraction, and under estimate the products; but all monitored species' mass fraction are better evaluated at stoichiometry, and the predictivity improves greatly when either pressure and/or temperature increases.

The H radical seems to be the least well estimated quantity, especially in rich configurations where, on the contrary, the other radicals are better evaluated.

 $PREMIX\ Validation$: The one dimensional free propagating flame simulation performed has the following specifications:

$$\phi = 1
P = 1 atm
T_e = 473 K$$

Globally, the results are really good, except for the gas velocity which is greatly over predicted with the skeletal scheme. The temperature graphs are almost overlapping.

In the case of the main reactants and products' mass fractions, we see on the "zoomed" areas that a small difference is present at the beginning, revealing a difference in the initialization process which is thought to be due to the way that the program calculates an equilibrium initial solution. However, even with these small errors, the mass fractions' drops and final values are very well predicted.

Discussion: In view of these first comparisons, it seems that the "beta version" of this semi-automated reduction process rapidly produced consistent results, in a very limited number of operations. It is very impressive that such a dramatic reduction in the number of species (from 225, originally, to only 91 for the 15/25 PCAF 0.950 mechanism) and reactions (from over 3000 originally, to about 400 for the 15/25 PCAF 0.950 mechanism) still be able to reproduce quite accurately most quantities of interest. It appears that, for a limited application range, a tremendous reduction of the initial mechanism could theoretically be obtained.

6 Conclusion

In recent years, efforts have been made towards a more accurate inclusion of chemistry in CFD simulations of combustion devices, allowed by the ever growing computer capabilities, in order to increase the prediction capabilities of simulations concerning, for example, pollutant emissions. The latest approach makes use of analytically derived reduced schemes, typically composed of under 50 global reactions, which differ from global schemes in that they do not require any adaptation to particular cases inside their respective parameter range.

This 6 month project was concerned with the different tools and methodologies used nowadays in the community to derive analytically reduced schemes from initial detailed or skeletal ones. The work performed can be summarized as follows:

- Literature review of mathematical techniques available for the reduction of kinetic models;
- Description of the options offered by the open-source FORTRAN 77 program KINALC, specialized in the implementation of mathematical techniques for the reduction of kinetic models;
- KINALC tests on two different oxidation mechanisms (Methane/Air [24] and Kerosene/Air [27]) along with a validation of the various results
- Semi automatization of the KINALC reduction procedure, applied to the particular case of the PCAF option on CHEMKIN-II PSR results.

Globally it can be said that KINALC is a very efficient tool, provided that its original implementation is slightly modified so as to be able to post-process a large enough number of CHEMKIN results. Furthermore, as seen on the literature review, care must be taken when applying some of its options: sometimes, more "up-to-date" procedures are available, as it was the case for the detection of the large eigenvector elements in section 5.2. KINALC is, after all, a relatively "old" program.

It is necessary to emphasize also the fact that, even by reducing a large kinetic mechanism by a factor 2 or 3, it is still possible to retain most of the mechanism's information and therefore to perform an accurate study of combustion phenomena.

This last point, even if not "out of the blue", is crucial; as the next step to this study would be to develop an efficient reduction methodology for large hydrocarbon mechanisms, in order to obtain a Kerosene scheme sufficiently small to be used efficiently in global CFD tools, such as the CERFACS code AVBP for example. Such a reduction methodology would make use of the mathematical tools presented in this report, through the two necessary steps of an efficient reduction: the skeletal reduction and the more subtle analytical reduction. This is one of the objectives of the PhD thesis that I will be starting at CERFACS next January.

On a more personal note, I would like to conclude by addressing my thanks to all the people at CERFACS: seniors as well as PhD students, interns and staff, who have turned this 6 month experience into a career aspiration.

7 Annex

7.1 Annex A: Example of a detailed mechanism, the H2/O2 $San\ Diego$ mechanism

Reaction		$A^{\mathbf{a}}$	n	$E^{\mathbf{a}}$
$H + O_2 \rightleftharpoons OH + O$		3.52×10^{16}	-0.7	71.42
$H_2 + O \rightleftharpoons OH + H$		5.06×10^4	2.67	26.32
$H_2 + OH \rightleftharpoons H_2O + H$		1.17×10^{9}	1.3	15.21
$H_2O + O \rightleftharpoons 2OH$		7.06×10^{0}	3.84	53.47
$2H + M \rightleftharpoons H_2 + M^b$		1.30×10^{18}	-1.0	0.0
$H + OH + M \rightleftharpoons H_2O + M^b$		4.00×10^{22}	-2.0	0.0
$2O + M \rightleftharpoons O_2 + M^b$		6.17×10^{15}	-0.5	0.0
$H + O + M \rightleftharpoons OH + M^b$		4.71×10^{18}	-1.0	0.0
$O + OH + M \rightleftharpoons HO_2 + M^b$		8.30×10^{14}	0.0	0.0
$H + O_2 + M \rightleftharpoons HO_2 + M^c$	k_0	5.75×10^{19}	-1.4	0.0
	k_{∞}	4.65×10^{12}	0.44	0.0
$HO_2 + H \rightleftharpoons 2OH$		7.08×10^{13}	0.0	1.23
$HO_2 + H \rightleftharpoons H_2 + O_2$		1.66×10^{13}	0.0	3.44
$HO_2 + H \rightleftharpoons H_2O + O$		3.10×10^{13}	0.0	7.20
$HO_2 + O \rightleftharpoons OH + O_2$		2.00×10^{13}	0.0	0.0
$HO_2 + OH \rightleftharpoons H_2O + O_2$		2.89×10^{13}	0.0	-2.08
$2OH + M \rightleftharpoons H_2O_2 + M^d$	k_0	2.30×10^{18}	-0.9	-7.12
	k_{∞}	7.40×10^{13}	-0.37	0.0
$2HO_2 \rightleftharpoons H_2O_2 + O_2$		3.02×10^{12}	0.0	5.8
$H_2O_2 + H \rightleftharpoons HO_2 + H_2$		4.79×10^{13}	0.0	33.3
$H_2O_2 + H \rightleftharpoons H_2O + OH$		1.00×10^{13}	0.0	15.0
$H_2O_2 + OH \rightleftharpoons H_2O + HO_2$		7.08×10^{12}	0.0	6.0
$H_2O_2 + O \rightleftharpoons HO_2 + OH$		9.63×10^{6}	2.0	16.7

^aUnits are mol, s, cm³, kJ, and K.

Figure 15: The H2/O2 San Diego mechanism, as found in \ref{matrix} . Rate coefficients in Arrhenius form : $AT^n exp(-E/RT)$

 $[^]c\mathrm{Chaperon}$ efficiencies are 2.5 for H₂, 16.0 for H₂O, and 1.0 for all other species; Troe falloff with $F_c=0.5$

 $[^]b\mathrm{Chaperon}$ efficiencies are 2.5 for H₂, 12.0 for H₂O, and 1.0 for all other species.

^dChaperon efficiencies are 2.5 for H₂, 6.0 for H₂O, and 1.0 for all other species;

 $F_c = 0.265 \exp{(-T/94 \mathrm{K})} + 0.735 \exp{(-T/1756 \mathrm{K})} + \exp{(-5182 \mathrm{K}/T)}$

7.2 Annex B: A brief KINALC manual

The source code of KINALC has to be downloaded from the KINALC website (http://garfield.chem.elte.hu/Combustion/kinalc.htm) and compiled with subroutine dcklib.f of the CHEMKIN package. In a UNIX environment, the following command should be used:

qfortran -o kx kinalc.f dcklib.f

KINALC offers an important number of options, which can be classified by the type of analysis performed:

- Concentration sensitivity analysis
- Processing information from reaction rates and stoichiometry
- Providing kinetic information about the species

Fig. (2) shows a typical KINALC input Keyword file. It is a FORTRAN 77 entry file, easy to understand, where the order of lines does not matter. All keywords are reminded in this section, and can be found also inside the KINALC fortran file [47].

Keyworld for the source of data:

In the source of data, is specified the kind of computation that KINALC must post-process. Under CHEMKIN-II, the only available options are PSR, SENKIN and PREMIX.

Keyword for the additional information :

TIME \langle value \rangle : The mechanism is investigated at the concentrations (and possibly sensitivities) obtained at the time point(s) -seconds, given by this keyworld.

HEIGHT \langle value \rangle : The mechanism is investigated at the concentrations (and possibly sensitivities) obtained at the height(s) -in cm, given by this keyworld.

 $AT_{-}TEMP \ \langle \ value \ \rangle$: The mechanism is investigated at the concentrations (and possibly sensitivities) obtained at the temperature values - in K, given by this keyworld.

UNC REACTION #n \langle U \rangle or UNC ALL \langle U \rangle : Defines the uncertainty factor of coefficient of reaction n.

UNCH SPECIES #n \langle U \rangle or UNCH ALL \langle U \rangle : Defines the uncertainty factor of heat-of-formation of species n. Only with PREMIX

THEDY: Print detailed thermodynamic data.

COMMENTS: Print detailed comments on the analysis performed on the output file.

END: Closes the command list so that any subsequent command will be ignored.

```
!-----
! KINALC control file for the analysis of a
! stoichiometric CH4/air PSR application
!/ phi=1.2 atm=5 ASEN=> psr number 54ASEN
! source of data
CHEMKIN-II
PSR
SENKIN
PREMIX
! No further info necessary
! methods of analysis
!ROPAD
!TDLIM 100.
!ROPAB
!TBLIMS 3. 10. 100.
!CONNECT H2O
!LIFETIME
!QSSAS
!QSSAG H OH HO2
CSP 1.15E-4
COMMENTS
END
```

Figure 16: Example of a Keyword file for KINALC

Keyword for the concentration sensitivity analysis:

UNC_ANAL \langle spec1 \rangle \langle spec2 \rangle ... \langle T \rangle . The list concerns the species of interest. KINALC will perform uncertainty analysis based on local sensitivities (see section 3.2.1). It calculates the uncertainty of results based on the uncertainty of the reactions (or, with PREMIX only, on the uncertainty of the heat of formation of species), and will present the results in a statistical way by listing and ranking the importance of each reaction coefficient (or species, for heat of formation uncertainties) on the total uncertainty of the concentration of the i species of interest.

HSENS \langle spec1 \rangle \langle spec2 \rangle ... \langle T \rangle . The sensitivities of the concentrations of a chosen subset of species on the heat of formation of all species are calculated individually, and listed. Actually, the rows of a normalized "heat of formation sensitivity matrix" are printed out in descending order. This option can be used with PREMIX only.

SENS \langle spec1 \rangle \langle spec2 \rangle ... \langle T \rangle . The sensitivities of the concentrations of chosen species on all rate parameters of reactions are calculated individually, and listed. In fact, rows of the normalized sensitivity matrix S are printed out in descending order (see paragraph 3.2.1).

SENG \langle spec1 \rangle \langle spec2 \rangle ... \langle T \rangle . KINALC uses the overall concentration sensitivities (see 3.2.1) to measure the effects of parameter changes on the concentration of a group of species.

PCAS \langle spec1 \rangle \langle spec2 \rangle ... \langle T \rangle , along with **TPCAS** \langle TAS \rangle \langle TES \rangle . Identifies a reaction considered to have a large influence on species listed after PCAS, if present in a reaction group having an eigenvalue greater than TAS and characterized by an eigenvector element greater than TES. KINALC perform the mathematical PCA of matrix **S**. See 3.2.4 for further details.

Keyword for the analysis on reaction rates and stoichiometry:

RIMP \langle spec1 \rangle \langle spec2 \rangle , along with **TREAC** = x. Identifies important reaction by its estimation greater than x. KINALC assess the "importance of reactions" on the basis of an overall sensitivity of matrix **F** (see paragraph 3.2.1).

PCAF \langle nothing \rangle , along with **TPCAF** \langle TAS \rangle \langle TES \rangle . Identifies a reaction considered to have a large influence on important species, if present in a reaction group having an eigenvalue greater than TAS and characterized by an eigenvector element greater than TES. KINALC perform the mathematical PCA of matrix **F**.

ATOMFLOW \langle elem 1 \rangle \langle elem 2 \rangle , along with **FLUXVOUT**. Creates a text file, that contains the atom fluxes between species, and can be further visualized with JAVA program FluxViewer.

ROPAD, along with **TDLIM** \langle tdlim \rangle . "tdlim" represents a threshold for the least still listed contribution -it must be greater than 1/TDLIM of the most significant contribution. It gives a detailed and ranked list of reaction contributions to the production rates of the species of interest.

ROPAB, along with **BLIMS** \langle tblim1 \rangle \langle tblim2 \rangle \langle tblim3 \rangle . This option is exactly the same as ROPAD, only in a brief summary. The creation of the brief ROPA form is controlled by three values :

- Reactions, having contribution less than 1/TBLIM1 but greater than 1/TBLIM2 than the contribution of the greatest consuming/producing reactions, are given in parentheses.
- Reactions, having contribution less than 1/TBLIM2 than than the contribution of the greatest consuming/producing reactions, are omitted.
- All the consuming reactions are omitted, if the contribution of the greatest consuming reaction is less than 1/TBLIM3 than than the contribution of the greatest producing reaction.
- All the producing reactions are omitted, if the contribution of the greatest producing reaction is less than 1/TBLIM3 than than the contribution of the greatest consuming reaction.

 \mathbf{TROPA} : Effective in case of both \mathbf{ROPAD} and \mathbf{ROPAB} . A reaction is considered important if it has a higher contribution than TROPA % to the production rate of a species.

Keywords for the analysis that provide information about the species:

LIFETIME \langle spec 1 \rangle \langle spec 2 \rangle . KINALC prints the "chemical" lifetime of species. Actually, all it does is call a subroutine of the dcklib.f CHEMKIN-II library, which will calculate the destruction rate

depending on the current temperature and concentration of species (subroutine CKCTC in [12]).

CONNECT \langle spec1 \rangle \langle spec2 \rangle . This option provides the list of species having a close connection to a group of target species on the basis of the investigation of an overall sensitivity of the Jacobian (see paragraph 3.2.1).

QSSAS \langle spec 1 \rangle \langle spec 2 \rangle . This option provides an approximation of the error made on the final value of the concentration of an assumed QSSA species, when making that assumption. Refer to paragraph 3.3.1.

QSSAG \langle spec 1 \rangle \langle spec 2 \rangle . With this option, we get an approximation of the error made on the final value of the concentration of every assumed QSSA species, while taking into account that their error interact. For further details, refer to paragraph 3.3.1.

RALI \langle spec1 \rangle \langle spec2 \rangle . The identification of rate limiting steps for the production \rangle consumption of a given species i is based on the investigation of the time derivative of the concentration sensitivity matrix; hence on the matrix \mathbf{F} (see paragraph 3.2.1). Indeed, those steps are identified by high sensitivity gradient [44]. The i-th row of \mathbf{F} is then screened so as to find the highest value, and the 10 "top" reactions are listed along with their $\mathbf{F}_{i,j}$ value.

 $\mathbf{CSP}\ \langle\ \mathrm{tlcsp}\ \rangle$. "tlcsp" is the limiting time scale. This option performs a Computational Singular Perturbation analysis of the system, as explained in 3.3.2

7.3 Annex C: Automatisation of KINALC post-processing and application to the PCAF option

7.3.1 Summarizing scheme

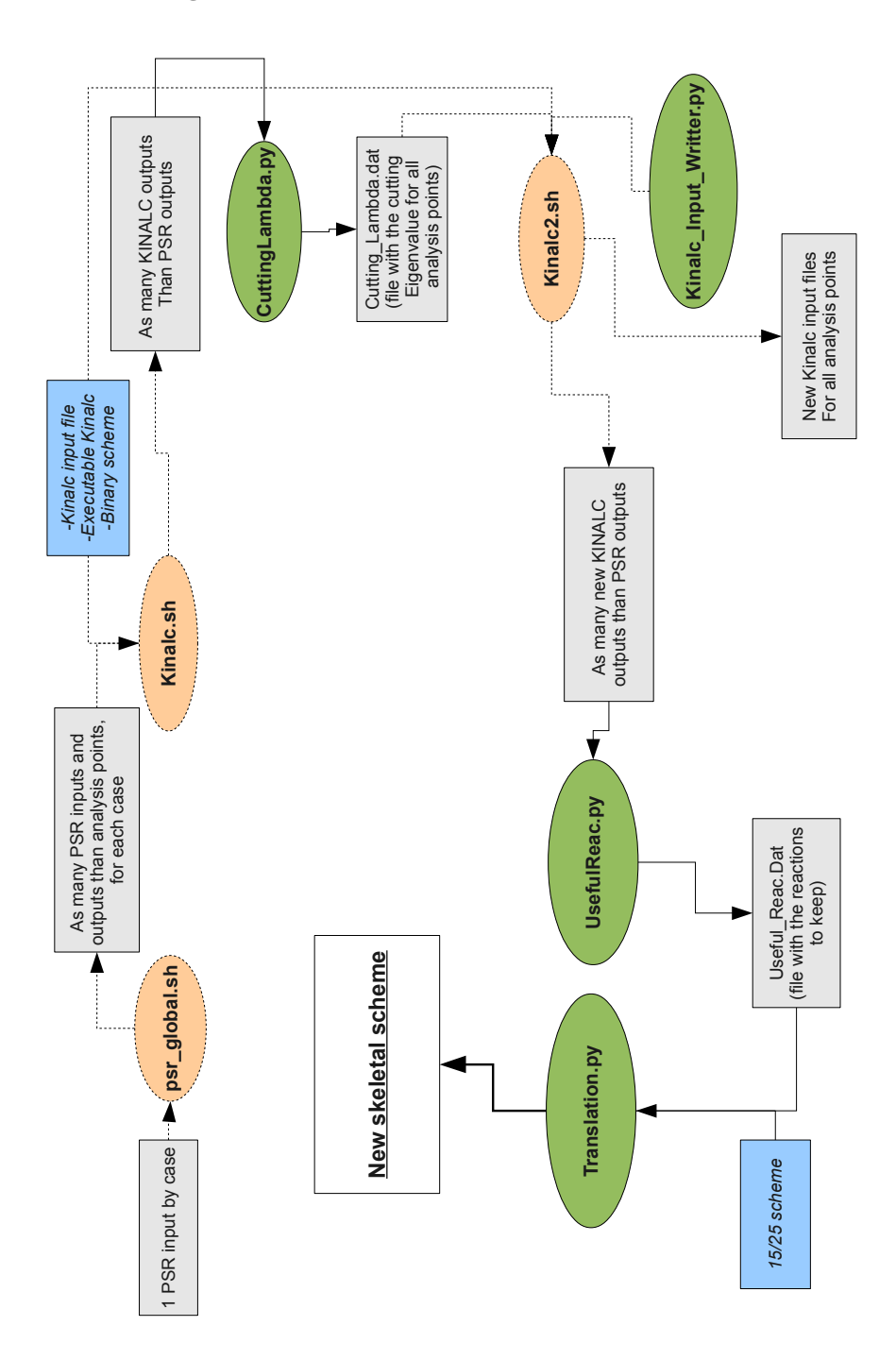


Figure 17: Semi-Automatisation of KINALC option PCAF with post-treatment

7.3.2 Modified KINALC driver

```
**********************
c
    * driver to program KINALC version 2.0
c
    * a CHEMKIN based program for kinetic analysis
c
c
c
   further info is in the comment lines of subroutine KINALC
   program driver
   implicit double precision (a-h, o-z), integer (i-n)
   parameter (leni = 5000000, lenr = 20000000, lenc = 20000,
           lensym = 16)
   dimension iw(leni), rw(lenr)
   character cw(lenc)*(lensym)
   character*10 fdflt
   character*80 fname, liname, llname, lsname, lrname, lmname
   character*11 ckiii,upcas
   logical isckiii, isck4
c
    lin = Unit number for control file input
   lkb = Unit number for standard input (e.g. keyboard)
c
   lscr = Unit number for standard output (e.g. screen)
    lout = Unit number for text output
С
    line = Unit number for CHEMKIN linking file input
    lnul = Unit number for discarded error messages
    ldata = Unit number for unformatted data input
    lfdata = Unit number for formatted data input
c
    leni = Length of integer work array
    lenr = Length of real work array
c
    lenc = Length of character work array
    lensym = Length of a character string in character work array
c
c
         = Integer work array
         = Real work array
   rw
c
        = Character work array
c
   data lin/4/, lkb/5/, lscr/6/, lout/7/, linc/8/, lnul/9/
   data ldata/10/, lfdata/11/, lfluxv/12/
   call getarg(1, lfname)
   call getarg(2, lrname)
   call getarg(3, lmname)
   call getarg(4, llname)
   call getarg(5, lsname)
```

```
write(lscr,200)
200 format(/////
        5x,'KINALC: Kinetic analysis of reaction mechanisms'//
   1
        5x,'A postprocessor program to CHEMKIN based',
   2
        1x,'simulation packages'//
   3
        5x,'Modified version for CHEMKIN-II ONLY:',
        5x, 'Input, output, mechanism, .last, .save'/
        5x,'Data files you gave to KINALC:'/)
    write (lscr ,*) liname, lrname, lmname, llname, lsname
    if (IARGC().ne.5) goto 263
C
    fname = liname
    open (unit = lin, status= 'old', form= 'formatted',
        file= fname, iostat= mes, err= 10)
C
    No CHEMKIN-III or CHEMKIN 4 mode of operation
c
c
    read(lin,211) ckiii
    ckiii=upcas(ckiii,11)
    isckiii=.false.
    isck4=.false.
C
    fname = lrname
    open (unit = lout, status= 'unknown', form= 'formatted',
        file= fname, iostat= mes, err= 10)
C
    fname = lmname
   open (unit = linc, status= 'old', form= 'unformatted',
        file= fname, iostat= mes, err= 10)
    fname = llname
    open (unit = ldata, status= 'unknown', form= 'unformatted',
        file= fname, iostat= mes, err= 10)
    fname = Isname
    open (unit = lfdata, status= 'unknown', form= 'formatted',
        file= fname, iostat= mes, err= 10)
    open (unit = lfluxv, status= 'unknown', form= 'formatted',
        file='fluxviewer.txt', iostat= mes, err= 10)
```

```
c
c
   UNIX
c
c
   open (unit = lnul, status='old', file='/dev/null')
c
    DOS / WINDOWS
c
c
    open (unit = lnul, status='old', file='NUL')
c
c-----PASS CONTROL TO KINALC-----
c
c
   call kinalc (lin,lout,linc,lnul,ldata,lfdata,lfluxv,
           leni, iw, lenr, rw, lenc, cw,isckiii,isck4)
   close (lin)
   close (lout)
   close (linc)
   close (ldata)
   close (Ifdata)
   stop
263 write (lscr, 266)
   stop
 10 write (lscr,210) mes,fname
   stop
266 format(
  1 ' WRONG NUMBER OF ARGUMENTS '//
             --- PROGRAM TERMINATED ---')
210 format(
   1 ' Error No',i4,' at opening file ',a10//
  2 '
             --- PROGRAM TERMINATED ---')
211 format(a11)
c
   end
```

7.3.3 Modified PCAF option of KINALC

```
subroutine pcaf(lout,kk,ii,nt,it,leniwk,lenrwk,
     1\ ickwrk, rckwrk, imp, nuki, ip, maxfon, if on, maxf, FT2,
     2 nthf,thf,t,c,wdot,q,b,fTf,e,es,smwt,y,dn,pres,rname,comments)
     implicit double precision (a-h, o-z), integer (i-n)
     parameter (lenistr=40)
     dimension ickwrk(leniwk),nuki(kk,ii),imp(ii,nt),ip(ii)
     dimension rckwrk(lenrwk),c(kk),wdot(kk),q(ii),b(ii) dimension FT2(ii,ii), fTf(ii,ii), ifon(ii,maxfon),
     1 e(ii), thf(2,maxf)
     dimension es(kk), smwt(kk), y(kk), dn(ii)
     character*(*) rname(ii)
character*(lenistr) istr
     logical comments
    PRINTING THRESHOLDS
    tevapr eigenvalue threshold
    tevepr eigenvector threshold
c
     do 16 is=1,nthf
        tevapr=thf(1,is)
        tevepr=thf(2,is)
 16 continue
   generation of nuki, q, wdot
c
   nuki net stoichiometric matrix
c
    q rates of reactions (mole/(cm3**3*sec))
c
    wdot molar production rates
       - Temperature (K)
c
    t
        - Molar concentrations (mole/cm**3)
     call cknu(kk,ickwrk,rckwrk,nuki)
     call ckqc(t,c,ickwrk,rckwrk,q)
     call ckwc(t,c,ickwrk,rckwrk,wdot)
c
    RHO (g/cm3)
     call ckrhoc (pres, t, c, ickwrk, rckwrk, rho)
    volsp (m3/g)
     volsp=1./rho
    MEAN SPEC HEAT ergs/(g*K)
c
     call ckcty(c,ickwrk,rckwrk,y)
     call ckcpbs(t,y,ickwrk,rckwrk,hms)
c
     call ckhms(t,ickwrk,rckwrk,es)
```

```
c
    MOLAR WEIGHTS (g/mol)
c
     call ckwt(ickwrk,rckwrk,smwt)
c
   RAW T production rate
c
     SUM = 0.
     DO 300 \text{ K} = 1, \text{ KK}
       K1 = K-1
       SUM = SUM + es(k) * wdot(k) * smwt(k)
300 CONTINUE
     delta = volsp *SUM /hms
c
   NORMALIZED T production rate
c
     do 301 i=1,ii
       sum=0
       do 302 k=1,kk
          sum=sum+es(k)*smwt(k)*dble(nuki(k,i))
302
        continue
        dn(i)=volsp*q(i)*sum/delta
301 continue
c
c
     do 1 i=1,ii
     do 1 j=1,i
     fTf(i,j)=0.
     do 1 k=1,kk+1
     if (k.eq.kk+1) then
       fki=dn(i)
       fkj=dn(j)
     else
       if (dabs(wdot(k)).lt.1.d-100) goto 1
       fki=dble(nuki(k,i))*q(i)/wdot(k)
       fkj = dble(nuki(k,j))*q(j)/wdot(k)
     endif
     fTf(i,j)=fTf(i,j)+fki*fkj
     FT2(i,j)=fTf(i,j)
     continue
 1
c
    eigenvectors (in fTf) and eigenvalues
c
    (vector q) by the SDIAG2 routine
c
c
     call sdiag2(ii,ii,fTf,q,e)
c
    do 7 i=1,ii
     imp(i,it)=0
     do 7 j=1,max fon
     ifon(i,j)=0
c
```

```
the principal components
     write(lout,200)
     do 5 i=1,ii
     if(q(i).lt.tevapr) goto 5
     write(lout,201) i,q(i)
     call order (ii,ip,fTf(1,i),b,e)
     somme = 0.
     do 4 j=1,ii
     somme = somme + b(j)*b(j)
     if(somme.gt.tevepr) goto 5
     write(lout,202) j,b(j),ip(j),rname(ip(j))
     imp(ip(j),it) = imp(ip(j),it) + 1
     ifon(ip(j),imp(ip(j),it)) = i
     continue
 5
     continue
    choosing the thresholds for mechanism reduction
c
c
     write(lout,210)
 15 continue
 11 write(lout,205) tevapr,tevepr
     do 12 i=1,ii
     istr= rname(i)
     if(imp(i,it).eq.0) then
        write(lout,206) i,istr(:20)
               else
        write(lout,206) i,istr(:20),(ifon(i,j),j=1,imp(i,it))
               endif
 12 continue
c
     if (comments) write(lout,209)
c
   FORMATS
c
c
200 format (//' ==== PCAF ===
                                                                           =='///5x,
   1 'Principal component analysis of the rate sensitivity matrix:'
201 format(//3x,'No',i4,' eigenvalue :',1pe15.5/9x,' eigenvector :'/)
202 format(5x,i5,1pe15.5,i5,2x,a40)
205 format(/' ------
         /2x,' Threshold value for eigenvalues:',1pe15.3,
  1
         /2x,' Threshold value for eigenvectors:',0pf12.3//
  2
         /6x,' reactions',16x,'reaction groups')
206 format(1x,i5,1x,a20,3x,20i3.0,5(/30x,20i3.0))
209 format(//
   1 'The numbers after the reactions show',
  2' which reaction groups'/
   3 ' (revealed by the eigenvalue-eigenvector analysis)'/
```

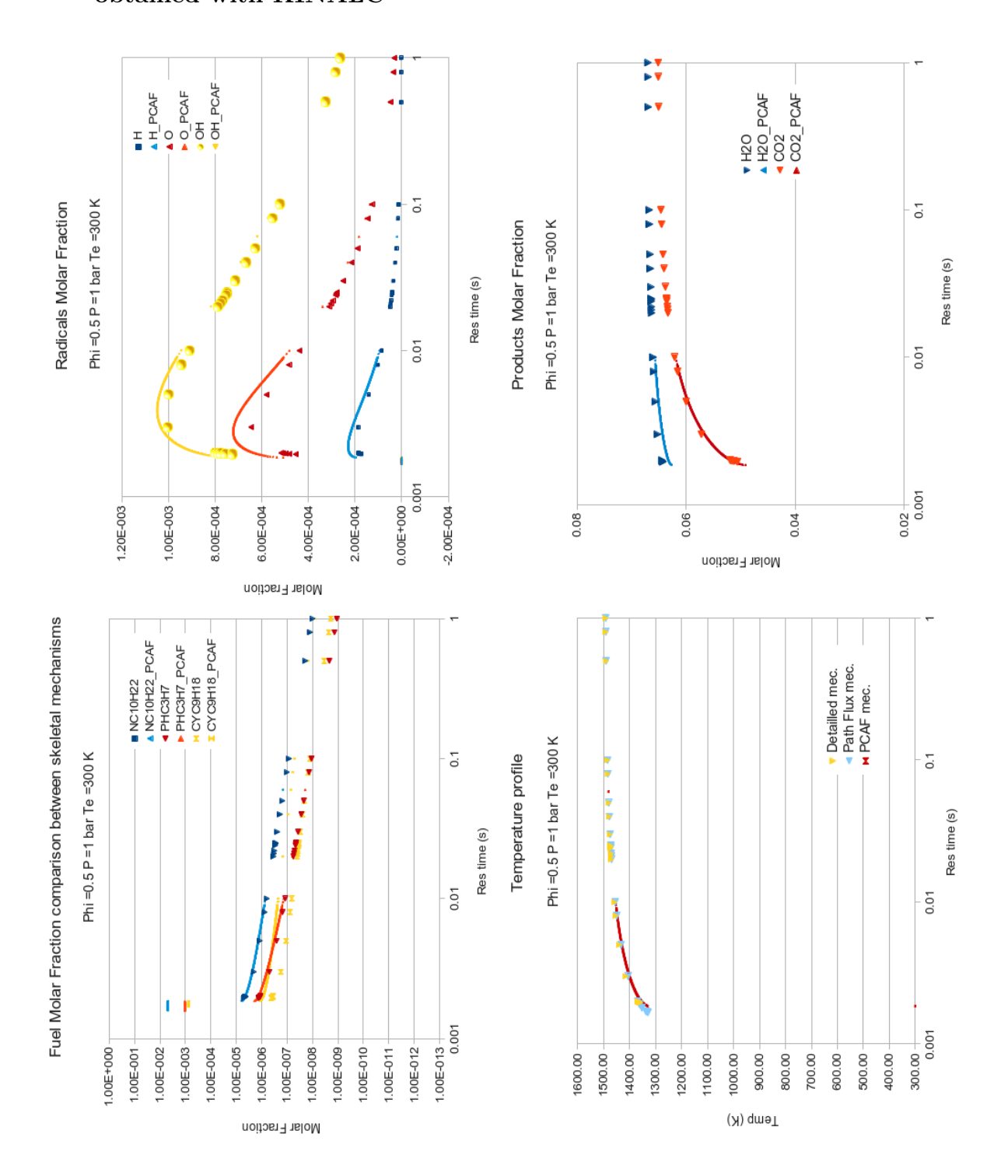
```
4 ' the reaction is a member of. The indicated'/
5 ' reaction groups are characterized by high eigenvalues'/
6 ' (i.e. higher than the threshold for eigenvalues).'/
7 ' Only reactions, having high weight in a reaction group'/
8 ' (i.e. higher than the threshold for eigenvector '/
9 ' elements) are indicated.'//
a ' Assessment of the importance of reactions based on '/
b ' the principal component analysis of matrix F'/
c ' see Turanyi et al., Int.J.Chem.Kinet.,21,83-99(1989)'//)
210 format(//2x,' Relation of reaction groups to reactions'//)
c return
end
```

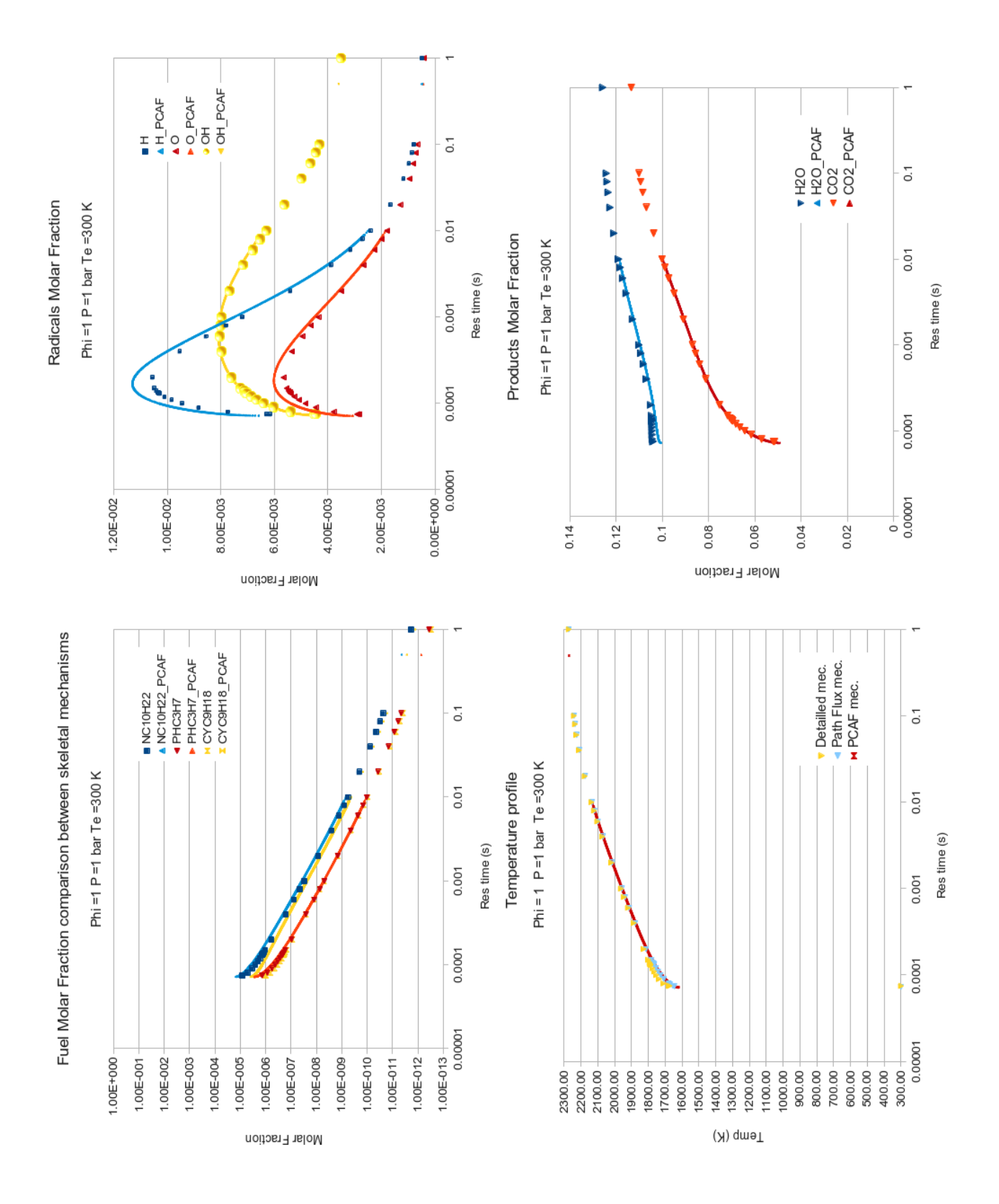
7.3.4 Link to the python programs (for CERFACS people)

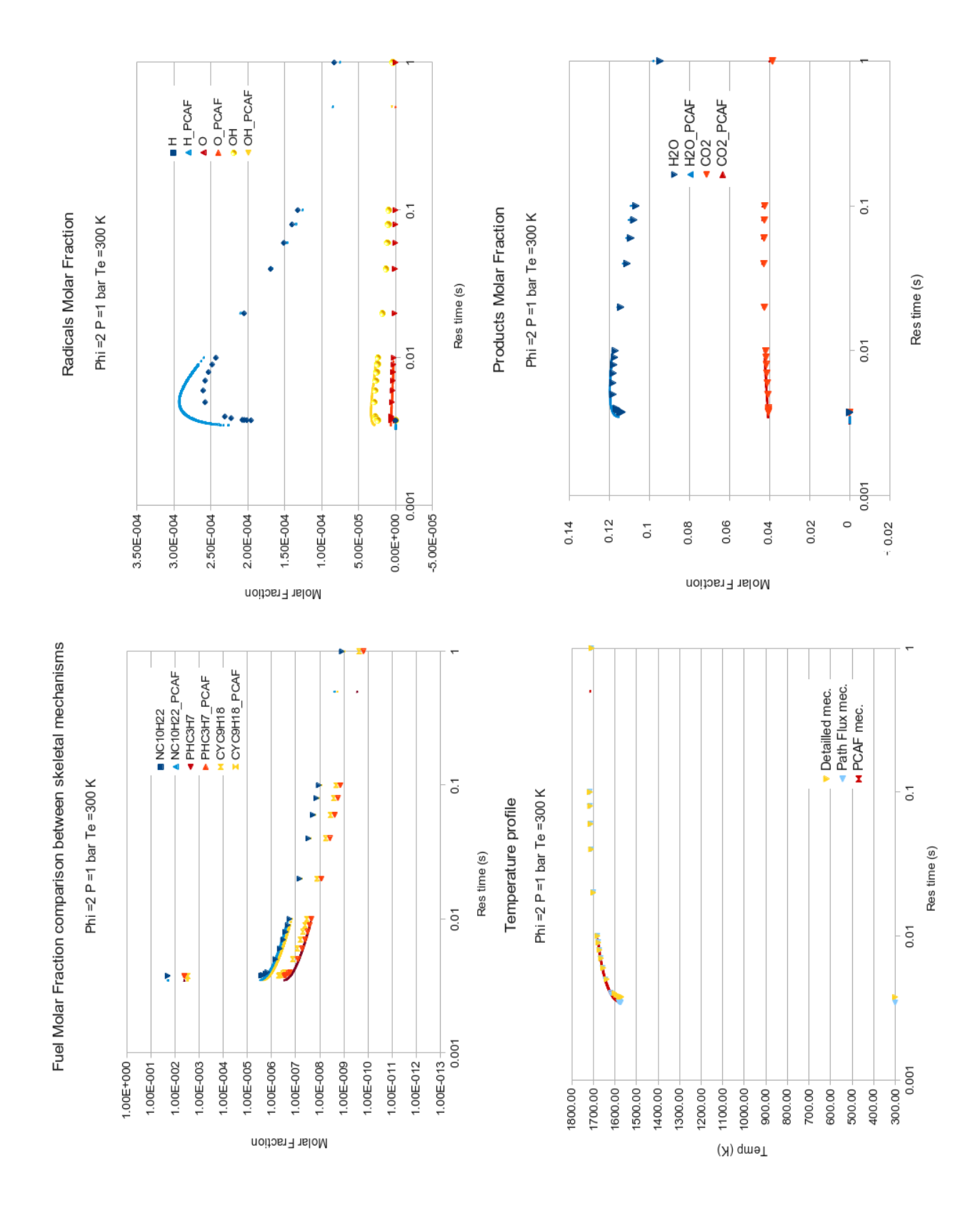
Link to the shell scripts and associated python programs involved in the automatization of the PCAF option, in the order of their utilization in the gobal scheme (see fig. (17)):

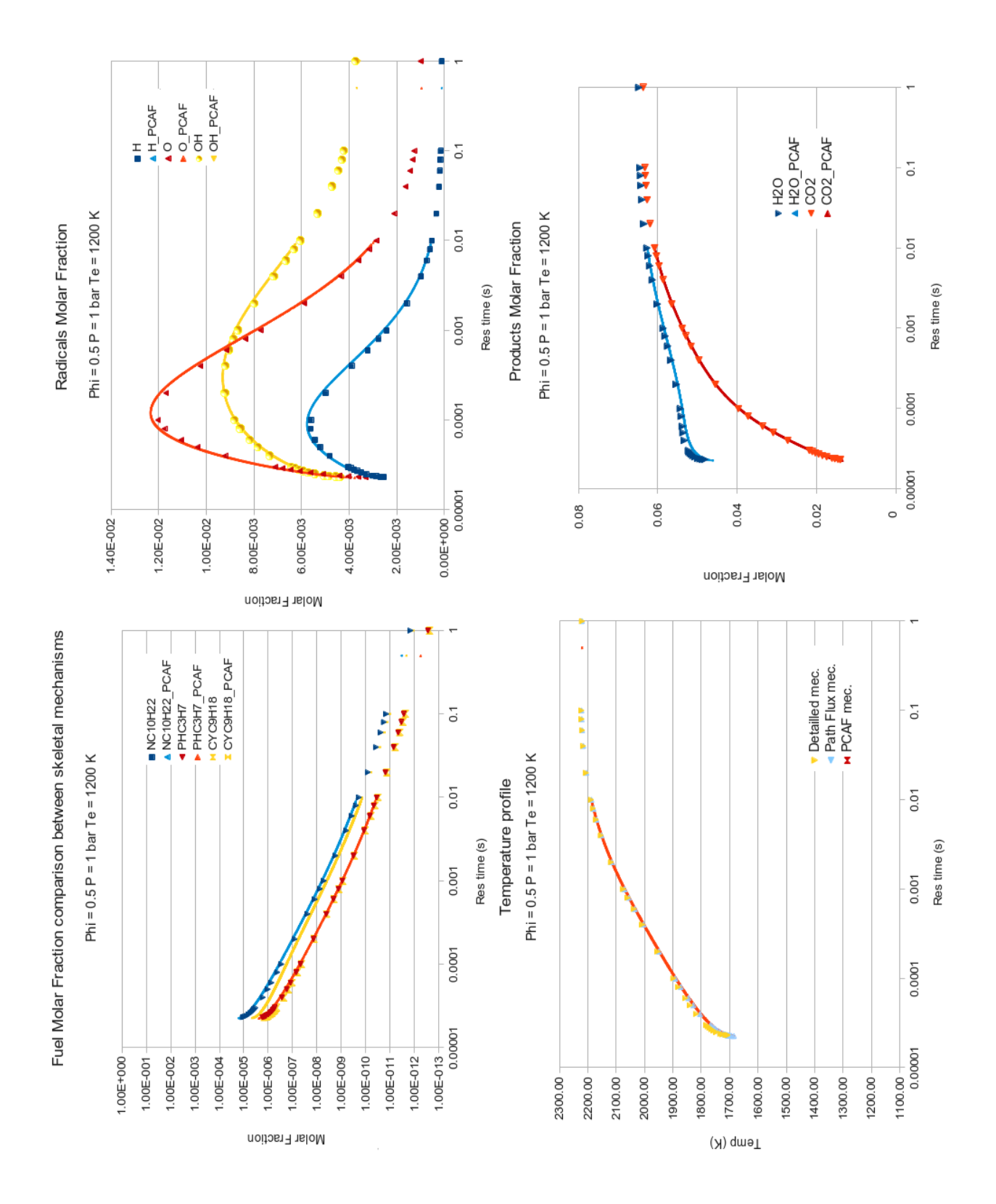
- \bullet psr_global.sh : /wkdir/stg-cfds/felden/CHEMKIN_V2_KINALC_gfortran/KEROSENE_Anne/PSR_Kinalc
- \bullet Kinalc.sh : /wkdir/stg-cfds/felden/CHEMKIN_V2_KINALC_gfortran/KEROSENE_Anne /PSR/PSR_Kinalc/Resultats_KINALC_PCAF
- \bullet Cutting Lambda.py : /wkdir/stg-cfds/felden/CHEMKIN_V2_KINALC_gfortran/KEROSENE_Anne/PSR/PSR_Kinalc/Resultats_KINALC_PCAF/Kinalc_PostPCAF
- $\bullet \ \, \text{Kinalc_Input_Writter.py}: \\ / wkdir/stg-cfds/felden/CHEMKIN_V2_KINALC_gfortran/KEROSENE_Anne \\ / PSR/PSR_Kinalc/Resultats_KINALC_PCAF/KINALC_tools \\$
- Kinalc2.sh: /wkdir/stg-cfds/felden/CHEMKIN_V2_KINALC_gfortran/KEROSENE_Anne /PSR_Kinalc/Resultats_KINALC_PCAF
- Useful Reactions.py : /wkdir/stg-cfds/felden/CHEMKIN_V2_KINALC_gfortran/KEROSENE_Anne/PSR/PSR_Kinalc/Resultats_KINALC_PCAF/Kinalc_PostPCAF
- $\bullet \ \, Schema Writter.py: /wkdir/stg-cfds/felden/CHEMKIN_V2_KINALC_gfortran/KEROSENE_Anne/PSR/PSR_Kinalc/Resultats_KINALC_PCAF/Kinalc_PostPCAF \\$

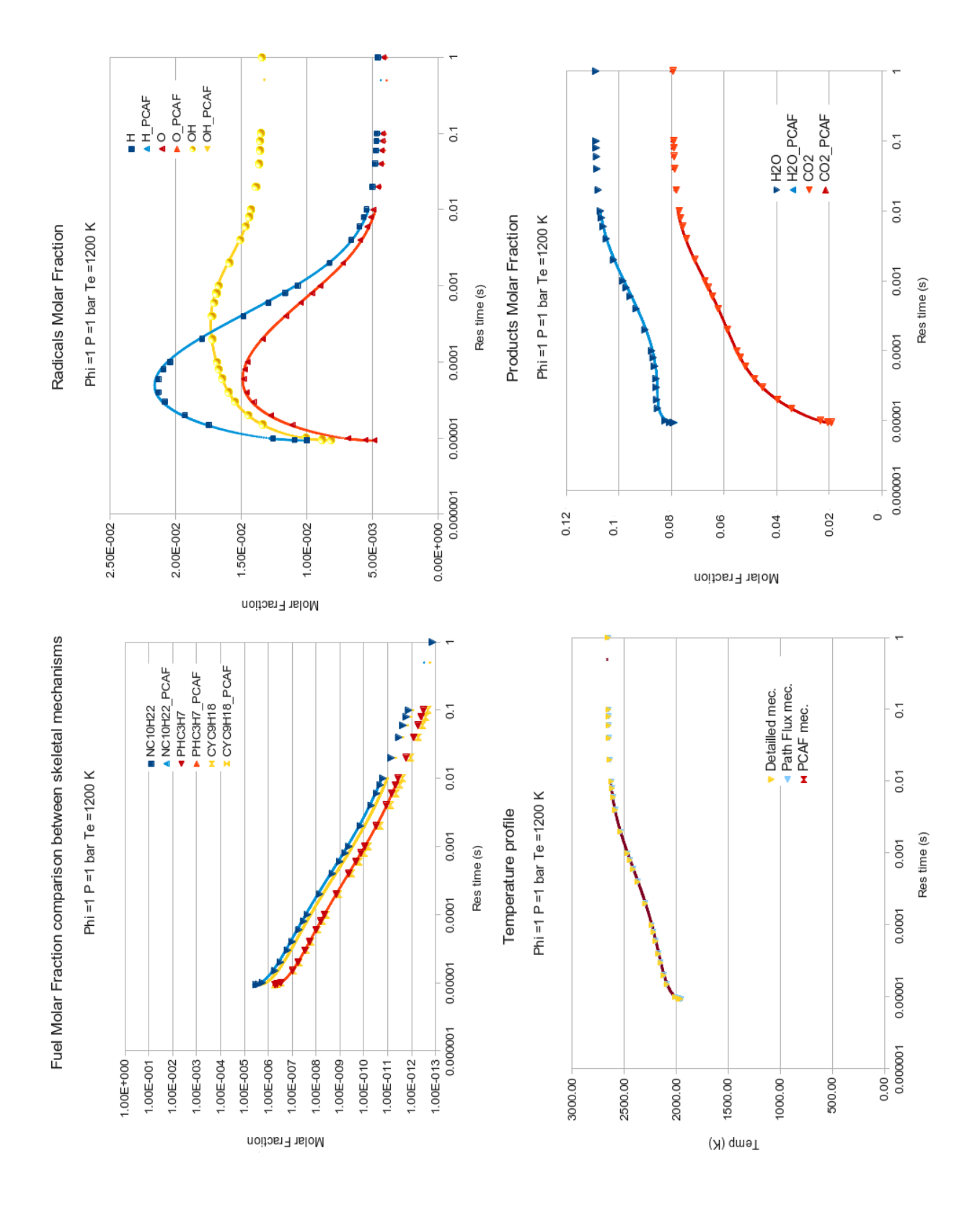
7.4 Annex D: PSR validation of the skeletal 15/25 PCAF-0.950 mechanism obtained with KINALC

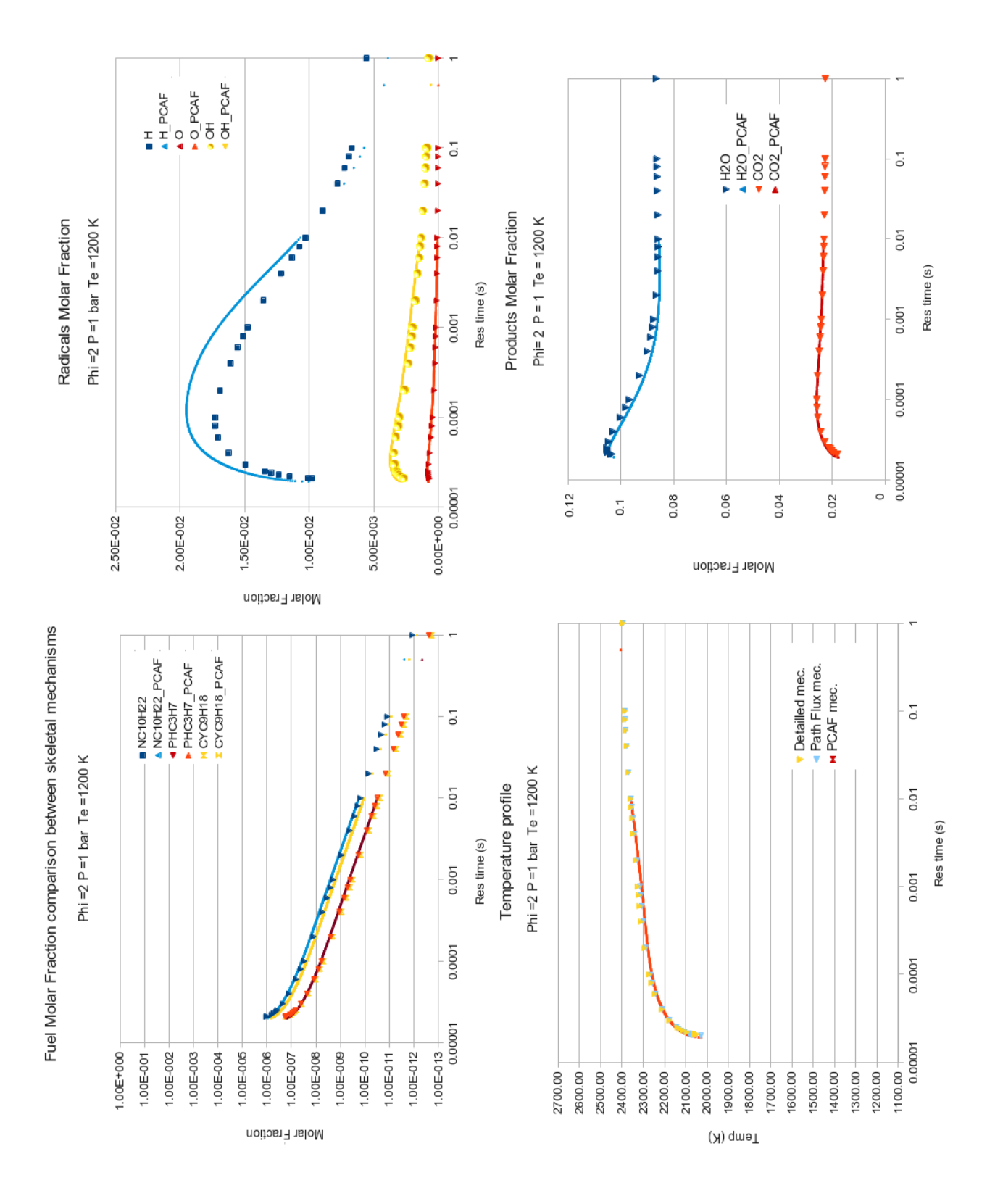


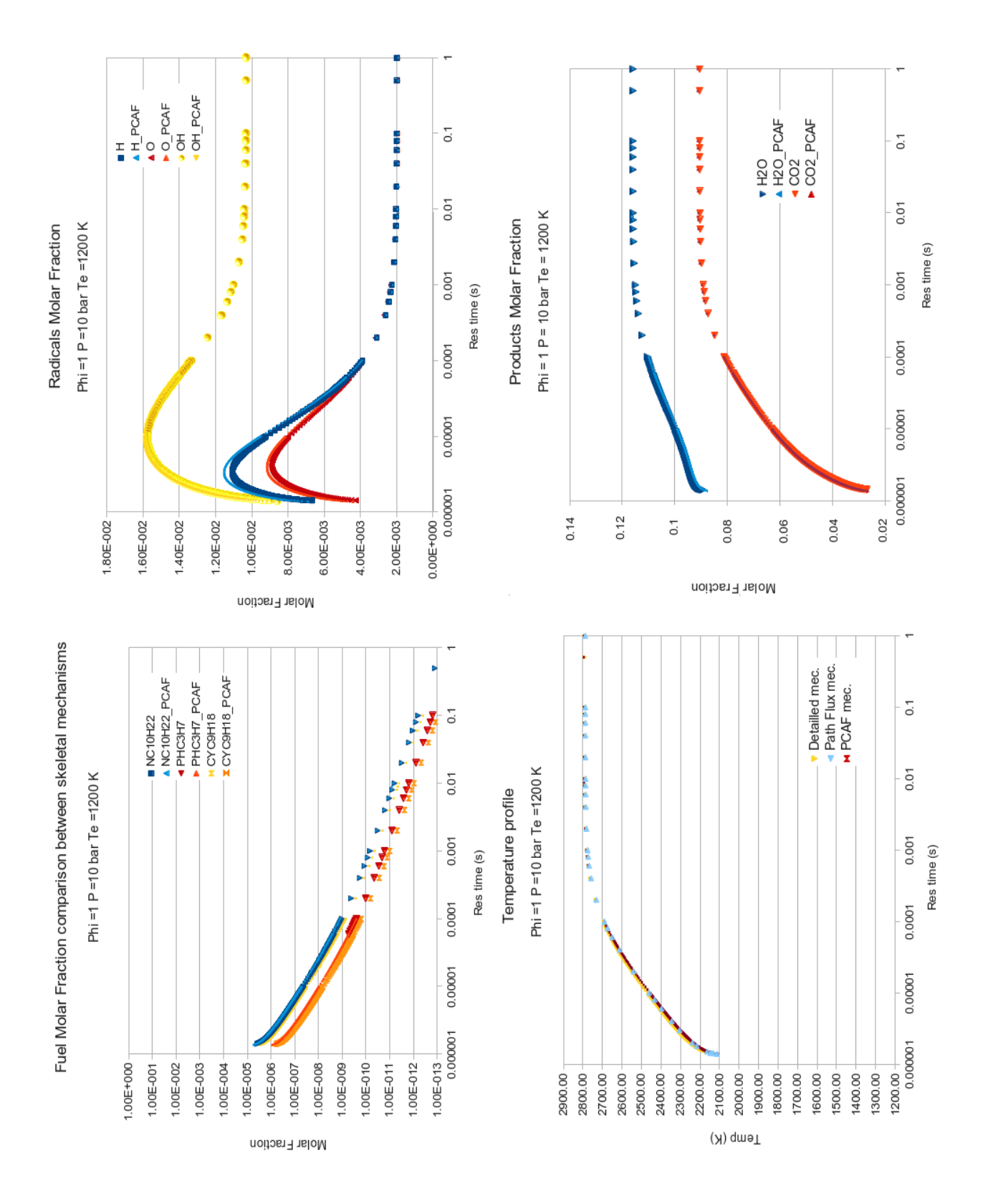












P = 1 atm

Rel Error (%)

157.94

5.13

P = 1 atm							
Te = 300 K				Te = 600 K			
Phi	0.5	1	2	Phi	0.5	1	2
PIII	0.5	ı	2	FIII	0.5	- 1	2
T extinction				T extinction			
Detailed mec.	1358.55	1673.72	1570.26	Detailed mec.	1469.47	1752.72	1747.43
Path Flux mec.	1329.77	1644.81	1572.83	Path Flux mec.	1432.65	1729.30	1741.74
PCAF mec.	1330.68	1618.71	1574.97	PCAF mec.	1425.68	1715.89	1741.50
Rel Error (%)	2.12	1.73	0.16	Rel Error (%)	2.51	1.34	0.33
Rel Error (%)	2.05	3.29	0.30	Rel Error (%)	2.98	2.10	0.34
Tau extinction				Tau extinction			
Detailed mec.	1.95E-003	7.48E-005	3.76E-003				
Path Flux mec.	1.67E-003	7.30E-005	3.45E-003	Path Flux mec.	2.58E-004	3.68E-005	4.93E-004 4.47E-004
PCAF mec.	1.85 E- 003	7.18 E- 005	3.48E-003	PCAF mec.			
Rel Error (%)	14.36	2.41	8.24	Rel Error (%)	2.61E-004	3.64E-005	4.29E-004 9.33
× /				X /	9.15	0.81	
Rel Error (%)	5.13	4.01	7.45	Rel Error (%)	8.10	1.89	12.98
Te = 900 K Te = 1200 K							
Phi	0.5	1	2	Phi	0.5	1	2
					'	'	
T extinction				T extinction			
Detailed mec.	1582.65	1861.34	1913.19	Detailed mec.	1707.11	1959.60	2048.81
Path Flux mec.	1543.38	1845.98	1904.53	Path Flux mec.	1684.73	1949.55	2028.63
PCAF mec.	1542.22	1840.39	1906.24	PCAF mec.	1683.94	1946.39	2027.2
Rel Error (%)	2.48	0.83	0.45	Rel Error (%)	1.31	0.51	0.98
Rel Error (%)	2.55	1.13	0.36	Rel Error (%)	1.36	0.67	1.05
Tau extinction				Tau extinction			
Detailed mec.	7.29E-005	1.86E-005	7.71E-005	Detailed mec.	2.31E-005	9.39E-006	2.08E-005
Path Flux mec.	6.82 E- 005	1.85 E- 005	7.17 E- 005	Path Flux mec.	2.25 E- 005	9.36E-006	1.99E-005
PCAF mec.	6.80E-005	1.84E-005	6.77 E- 005	PCAF mec.	2.25 E- 005	9.31E-006	1.91E-005
Rel Error (%)	6.45	0.54	7.00	Rel Error (%)	2.60	0.32	4.33
Rel Error (%)	6.72	1.08	12.19	Rel Error (%)	2.60	0.85	8.17
P = 10 atm							
Te = 300 K				Te = 1200 K			
Te - 500 K				Te = 1200 K			
Phi	0.5	1	2	Phi	0.5	1	2
T extinction				T extinction		<u>, </u>	
Detailed mec.	1392.61	1871.27	1605.03	Detailed mec.	1829.91	2127.64	2147.25
Path Flux mec.		1893.58		Path Flux mec.		2112.72	
PCAF mec.	1388.46	1857.83	1616.17	PCAF mec.	1809.33	2107.69	2131.77
Rel Error (%)	0.20	1.19	0.60	Rel Error (%)	4.40	0.70	0.70
Rel Error (%)	0.30	0.72	0.69	Rel Error (%)	1.12	0.94	0.72
Tau extinction	5 0 4 5 0 0 0	4 505 005	C 04E 004	Tau extinction	1	4 405 000	5 70E 000
Detailed mec.	5.04 E- 003	1.56E-005	6.81E-004	Detailed mec.	5.21E-006		5.70E-006
Path Flux mec.	4 205 000	1.50E-005	6.045.004	Path Flux mec.		1.39E-006	- 44 - 44
PCAF mec.	1.30E-002	1.48E-005	6.84 E- 004	PCAF mec.	4.94E-006	1.37E-006	5.19 E- 006
Rel Error (%)		3.85		Rel Error (%)		2.11	

N.B.: The 4 cases P=10 atm, $\phi=0.5$ and 2, $T_e=300$ and 1200 K where not part of the original parameter range, but were tested with the new skeletal PCAF mechanism.

0.44 Rel Error (%)

3.52

P = 3 atm

Te = 300 K

Phi	0.5	1	2	Phi	0.5	1	2

T extinction

1 CAUTOUOTI			
Detailed mec.	1400.56	1761.41	1589.12
Path Flux mec.	1398.70	1728.66	1591.24
PCAF mec.	1400.60	1719.46	1596.26
Rel Error (%)	0.13	1.86	0.13
Rel Error (%)	0.00	2.38	0.45

T extinction

Detailed mec.	1530.26	1842.38	1744.65
Path Flux mec.	1504.59	1805.34	1742.87
PCAF mec.	1503.06	1797.48	1746.91
Rel Error (%)	1.68	2.01	0.10
Pel Frror (%)	1 72	2 44	0.13

Tau extinction

Detailed mec.	2.32E-003	3.23E-005	1.86E-003
Path Flux mec.	2.48E-003	3.13E-005	1.79E-003
PCAF mec.	2.89E-003	3.07E-005	1.81E-003
Rel Error (%)	6.90	3.10	3.76
Rel Error (%)	24.57	4.95	2.69

Tau extinction

Detailed mec.	1.80E-004	1.53E-005	3.06E-004
Path Flux mec.	1.70E-004	1.49E-005	2.87E-004
PCAF mec.	1.76E-004	1.47E-005	2.82E-004
Rel Error (%)	5.56	2.61	6.21
Rel Error (%)	2.22	3.92	7.84

Te = 900 K

BL:	0.5	4	_
Pni	0.5	1	2

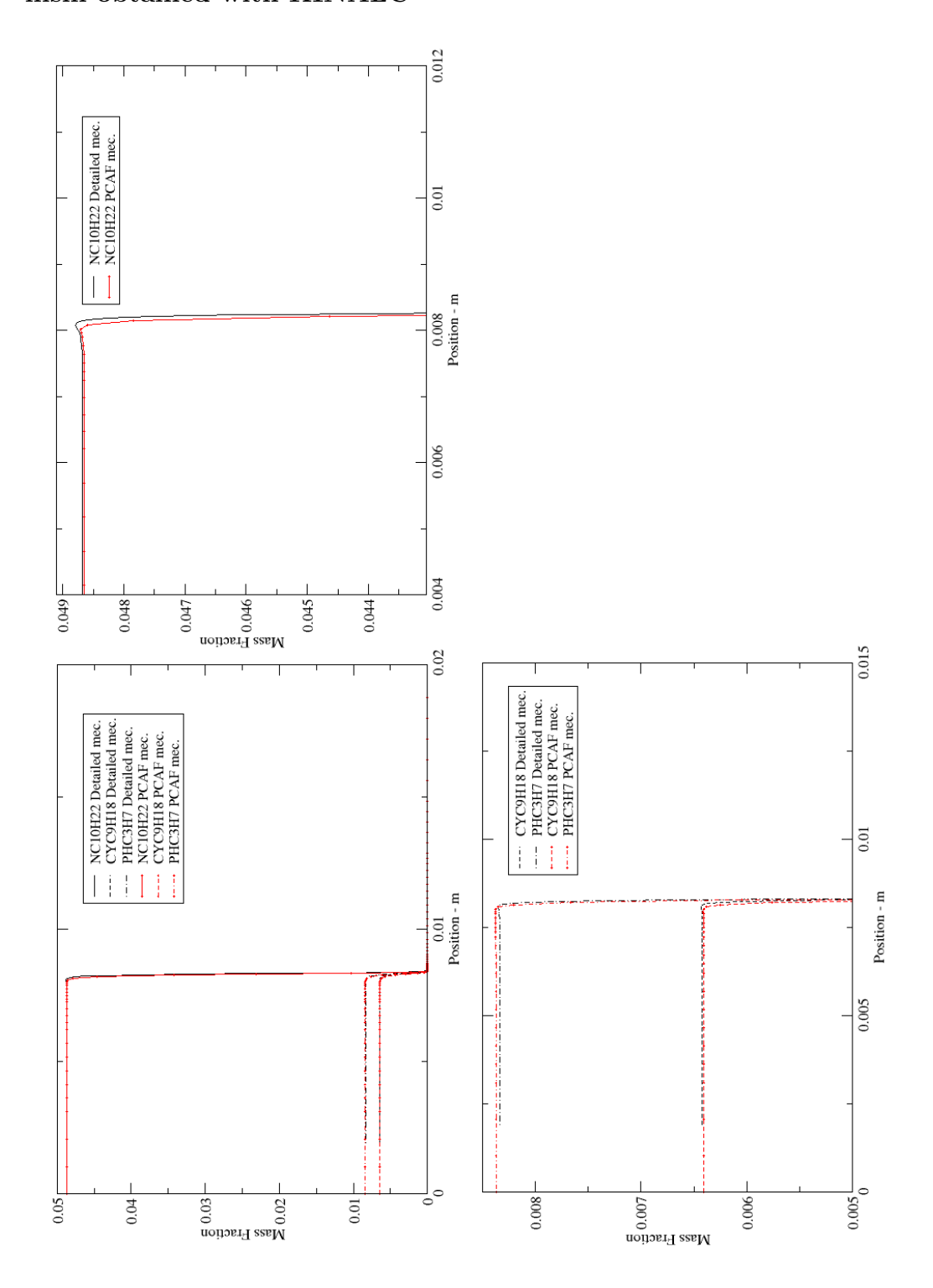
T extinction

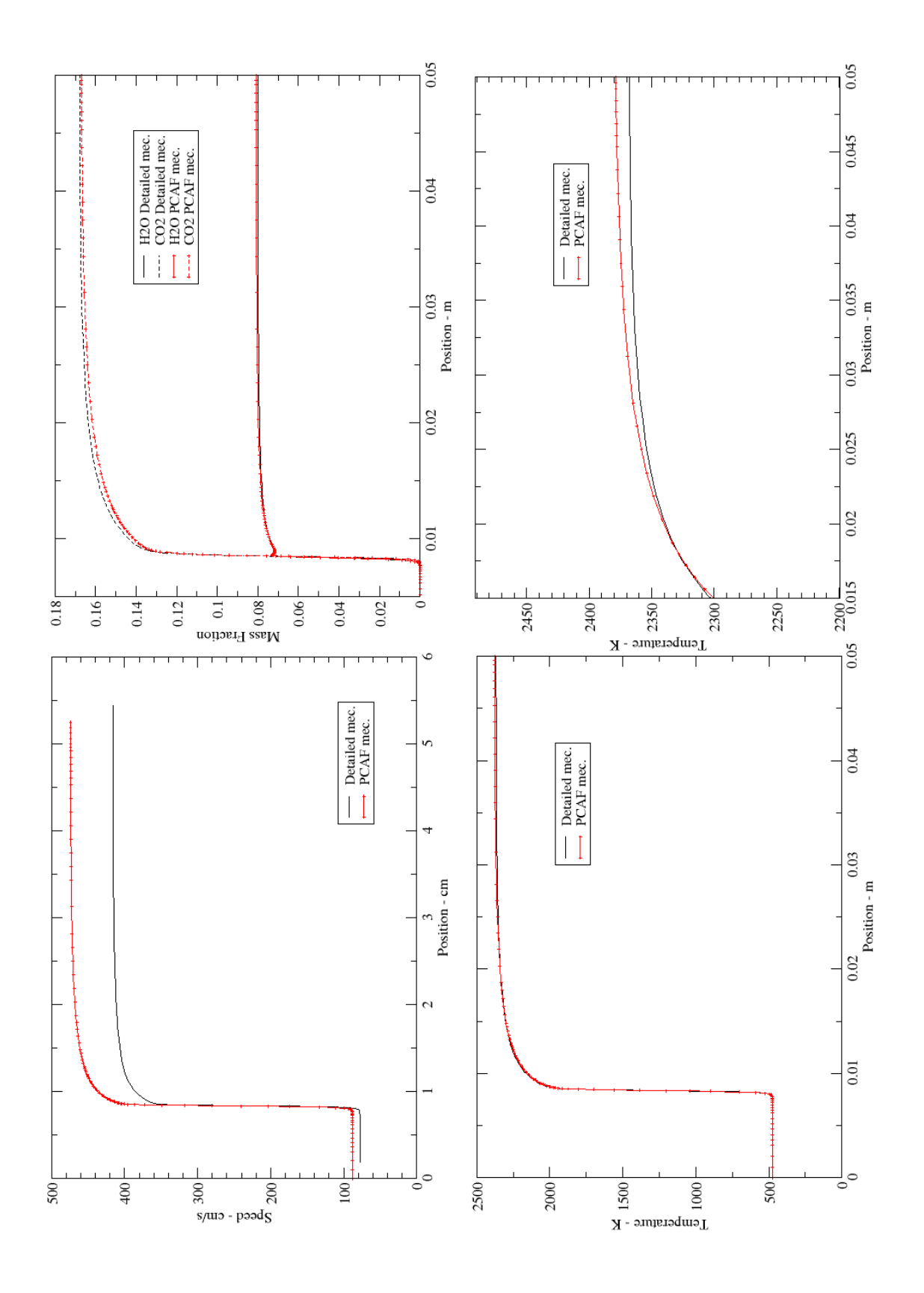
Detailed mec.	1639.30	1923.19	1944.18
Path Flux mec.	1611.63	1901.09	1927.85
PCAF mec.	1604.87	1894.48	1936.23
Rel Error (%)	1.69	1.15	0.84
Rel Error (%)	2.10	1.49	0.41

Tau extinction

Detailed mec.	3.64E-005	7.40E-006	4.73E-005
Path Flux mec.	3.43E-005	7.28 E -006	4.43E-005
PCAF mec.	3.43E-005	7.21 E- 006	4.19 E- 005
Rel Error (%)	5.77	1.62	6.34
Rel Error (%)	5.77	2.57	11.42

7.5 Annex E: PREMIX validation of the skeletal 15/25 PCAF-0.950 mechanism obtained with KINALC





References

- [1] P. Boivin. Reduced-Kinetic Mechanisms for Hydrogen and Syngas Combustion Including Autoignition. PhD thesis, University CARLOS III Madrid, 2011.
- [2] W. C. Chang. Modelling of Nitrogen Oxide Formation in Turbulent Flames: Development of Reduced Mechanisms and Mixing Models. Ph. d., University of California at Berkeley, 1995.
- [3] J.Y. Chen. Development of reduced mechanisms for numerical modelling of turbulent combustion. In Workshop on Numerical Aspects of Reduction in Chemical Kinetics, CERMICS-ENPC, Cite Descartes, Champus sur Marne, France, Reno, NV, 1997.
- [4] M.Ó Conaire, H.J. Curran, J.M. Simmie, W.J. Pitz, and C.K. Westbrook. A comprehensive modeling study of hydrogen oxidation. *International Journal of Chemical Kinetics*, 36:603–622, 2004.
- [5] P. Dagaut, M. Reuillon, J.-C. Boettner, and M. Cathonnet. Kerosene combustion at pressures up to 40 atm.: Experimental study and detailled chemical kinetic modeling. *Twenty-Fifth Symposium (International) on Combustion / The Combustion Institute*, pages 919–926, 1994.
- [6] G. Dixon-Lewis. Flame structure and flame reaction kinetics. ii. transport phenomena in multicomponent systems. Proc. Roy. Soc., A 307:111–135, 1968.
- [7] M. Frenklach, H. Wang, M. Goldenberg, G.P. Smith, D.M. Golden, C.T. Bowman, R.K. Hanson, W.C. Gardiner, and V. Lissianki. Gri-mech: an optimized detailed chemical reaction mechanism for methane combustion. Technical Report GRI-Report GRI-95/0058, Gas Research Institute, 1995.
- [8] C. E. Frouzakis and K. Boulouchos. Analysis and reduction of the ch4-air mechanism at lean conditions. *Combustion Science and Technology*, 159:281–303, 2000.
- [9] N.J. Glassmaker. Intrinsic low-dimensional manifold method forrational simplification of chemical kinetics. Technical report, University of Notre Dame, 1999.
- [10] J.F. Griffiths. Reduced kinetic models and their application to practical combustion systems. Progress in Energy and Combustion Science, 21:25–107, 1995.
- [11] D.M. Hamby. A review of techniques for parameter sensitivity analysis of environmental models. Environmental Monitoring and Assessment, 32:135–154, 1994.
- [12] R. J. Kee and al. Chemkin: A software package for the analysis of gas-phase chemical and plasma kinetics. Technical Report Based on SAND96-8216, Sandia National Laboratories, 2000.
- [13] R. J. Kee and al. Transport: A software package for the evaluation of gas-phase, multicomponent transport properties. Technical Report Based on SAND86-8246B, Reaction Design Inc., 2000.
- [14] R. J. Kee, J. F. Grcar, M. Smooke, and J. A. Miller. Premix: A fortran program for modeling steady laminar one-dimensional flames. Technical Report SAND85-8240, Sandia National Laboratories, 1985.
- [15] R.J. Kee, F.M. Rupley, and J.A. Miller. Chemkin-ii: A fortran chemical kinetics package for the analysis of gas-phase chemical kinetics. Technical Report SAND89-8009B, Sandia National Laboratories, 1989.
- [16] H.S. Lam and D.A. Goussis. Conventional asymptotics and computational singular perturbation for simplified kinetics modelling. Lecture Notes in Physics, 384:227–242, 1991.
- [17] H.S. Lam and D.A. Goussis. The csp method for simplifying kinetics. *International Journal of Chemical Kinetics*, 26:461–486, 1994.
- [18] V. Lepage. Elaboration d'une méthode de réduction de schémas détaillés. Application aux mécanismes de combustion du gaz naturel et du n-décane. Ph.d, Universite Paris VI, 2000.
- [19] J. Li, Z. Zhao, A. Kazakov, and F.L. Dryer. An updated comprehensive kinetic model of hydrogen combustion. *International Journal of Chemical Kinetics*, 36:566–575, 2004.
- [20] F.A. Lindemann. volume 17. 1922.

- [21] T. Lu. http://www.engr.uconn.edu/tlu/mechs/mechs.htm. 30 skeletal Methane-Air mechanism, 2008.
- [22] T. Lu, Y. Ju, and C.-K. Law. Complex csp for chemistry reduction and analysis. *Combustion and Flame*, 126:1445–1455, 2001.
- [23] T. Lu and C. K. Law. Systematic approach to obtain analytic solutions of quasi steady state species in reduced mechanisms. *Journal of Physical Chemistry*, 110:13202–13208, 2006.
- [24] T. Lu and C. K. Law. A criterion based on computational singular perturbation for the identification of quasi steady state species: A reduced mechanism for methane oxidation with no chemistry. *Combustion and Flame*, 154:761–774, 2008.
- [25] T. Lu and C. K. Law. Strategies for mechanism reduction for large hydrocarbons: n-heptane. Combustion and Flame, 154:153–163, 2008.
- [26] T. Lu, M. Plomer, Z. Luo, S.M. Sarathy, W.J. Pitz, S. Som, and D.E. Longman. Directed relation graph with expert knowledge for skeletal mechanism reduction. In 7th US National Combustion Meeting, 2011.
- [27] J. Luche. Obtention de modeles cinétiques réduits de combustion. Application à un mécanisme du kérosène. Phd thesis, Université d'Orléans, 2003.
- [28] A.E. Lutz, R.J. Kee, and J.A. Miller. Senkin: A fortran program for predicting homogeneous gas phase kinetics with sensitivity analysis. Technical Report SAND87-8248, Sandia National Laboratories, 1991.
- [29] U. Maas and S. B. Pope. Implementation of simplified chemical kinetics based on low-dimensional manifolds. *Proc. of the Combustion Institute*, 24:719 729, 1992.
- [30] U. Maas and S. B. Pope. Simplifying chemical kinetics: intrinsic low-dimensional manifolds in composition space. *Combustion and Flame*, 88:239 264, 1992.
- [31] A. Massias, D. Diamantis, E. Mastorakos, and D. A. Goussis. An algorithm for the construction of global reduced mechanisms with csp data. *Combustion and Flame*, 117:685–708, 1999.
- [32] E. Meeks, H. K. Moffat, J. F. Grear, and R. J. Kee. Aurora: A fortran program for modeling well stirred plasma and thermal reactors with gas and surface reactions. Technical Report SAND96-8218, Sandia National Laboratories, 1996.
- [33] M.A. Mueller, T.J. Kim, R.A. Yetter, and F.L. Dryer. Flow reactor studies and kinetic modeling of the h2/o2 reaction. *International Journal of Chemical Kinetics*, 31:113–125, 1999.
- [34] K. E. Niemeyer and C-J Sung. Drgep-based mechanism reduction strategies: graph search algorithms and skeletal primary reference fuel mechanisms. In AIAA Paper 2011-508, editor, 47st Aerospace Sciences Meeting including the New Horizons Forum and Aerospace Exposition, 2011.
- [35] N. Peters and B. Rogg. Reduced Kinetic Mechanisms for Applications in Combustion Systems. Lecture Notes in Physics. Springer Verlag, Heidelberg, 1993.
- [36] T. Poinsot and D. Veynante. Theoretical and numerical combustion, second edition. R.T. Edwards, 2005. out.
- [37] H. Rabitz, R. A. Yetter, and F. L. Dryer. A comprehensive reaction mechanism for carbon monoxide/hydrogen/oxygen kinetics. *Combustion Science and Techniques*, 79:97–128, 1991.
- [38] J.D. Ramshaw. Partial chemical equilibrium in fluid dynamics. Physics of Fluids, 23:675, 1980.
- [39] M. Rein. The partial equilibrium approximation in reacting flows. *Physics of Fluids A: Fluid Dynamics*, 4:873, 1992.
- [40] W. Sun, Chen Z., X. Gou, and Y. Ju. A path flux analysis method for the reduction of detailed chemical kinetic mechanisms. *Combustion and Flame*, 157:1298–1307, 2010.
- [41] C.J. Law C.K. Chen J.-Y. Sung. An augmented reduced mechanism for methane oxidation with comprehensive global parametric validation. In 27th Symposium (International) on Combustion, pages 295–304. The Combustion Institute, Pittsburgh, 1998.

- [42] A.S. TOMLIN, M.J PILLING, and T. TURANYI. Mechanism reduction for the oscillatory oxidation of hydrogen: Sensitivity and quasi-steady-state analyses. COMBUSTION AND FLAME, 91:107– 130, 1992.
- [43] T. Turanyi. Reduction of large reaction mechanisms. New Journal of Chemistry, 14:795–803, 1990.
- [44] T. Turanyi. Sensitivity analysis of complex kinetic systems. tools and applications. *Journal of Mathematical Chemistry*, 5:203–248, 1990.
- [45] T. Turanyi. Effect of the uncertainty of kinetic and thermodynamic data on methane flame simulation results. *Physical Chemistry Chemical Physics*, 4:2568–2578, 2002.
- [46] T. Turanyi, T. Bérces, and S. Vadja. Reation rate analysis of complex kinetic systems. *International Journal of Chemical Kinetics*, 21:83–99, 1989.
- [47] T. Turanyi, K.J. Hughes, M.J. Pilling, and A.S Tomlin. http://garfield.chem.elte.hu/combustion/kinalc.htm. KINALC website.
- [48] T. Turanyi, A.S. Tomlin, and M.J. Pilling. On the error of quasi-steady-state approximation. *Journal of Physical Chemistry*, 97:163–172, 1993.
- [49] T. Turanyi, L. Zalotai, S. Dobe, and T. Berces. Applications of sensitivity analysis to combustion chemistry. *Reliability Engineering and System Safety*, 57:41–48, 1997.
- [50] S. Vadja, P. Valko, and T. Turanyi. Principal component analysis of kinetic models. *International Journal of Chemical Kinetics*, 17:55–81, 1985.
- [51] M. Valorani and S. Paolucci. The g-scheme: A framework for multi-scale adaptive model reduction. Journal of Computational Physics, 228:4665–4701, 2009.
- [52] D. Veynante and T. Poinsot. Reynolds averaged and large eddy simulation modeling for turbulent combustion. In J. Ferziger O. Metais, editor, *New tools in turbulence modelling. Lecture 5*, pages 105–135. Les editions de Physique, Springer, 1997.
- [53] D. Voisin. Cinétique Chimique d'Oxydation d'Hydrocarbures et Obtention d'un Modéle pour la Combustion du Kéroséne. Ph.d, Université d'Orléans,, 1997.
- [54] F.A. Williams. Combustion theory. Benjamin Cummings, Menlo Park, CA, 1985.
- [55] J. Zador, I.Gy. Zsély, and T. Turanyi. Local and global uncertainty analysis of complex chemical kinetic systems. Reliability engineering and system safety, 91:1232–1240, 2006.